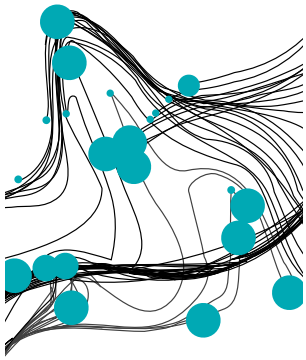

RAM ROBOTICS AND MECHATRONICS

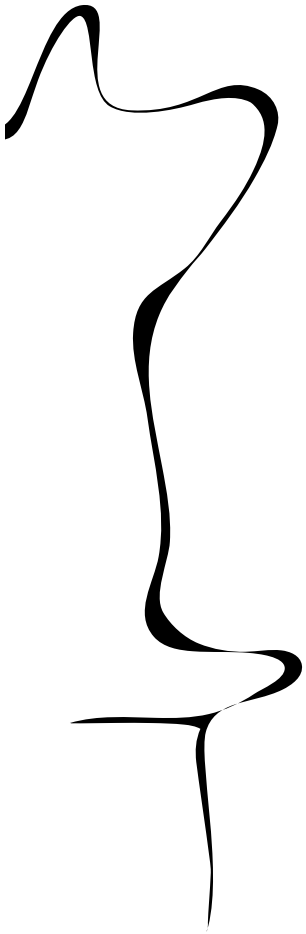

CATHETER MODELLING FOR MEDICAL SIMULATOR WITH CATHBOT INTEGRATION

R. (Rahul) Sriram

MSC ASSIGNMENT

Committee:
dr. ir. M. Abayazid
dr. G. Dagnino
dr. I.S.M. Khalil
dr. ir. W.M. Brink

July, 2024

047RaM2024
Robotics and Mechatronics
EEMCS
University of Twente
P.O. Box 217
7500 AE Enschede
The Netherlands

UNIVERSITY OF TWENTE. | TECHMED CENTRE
UNIVERSITY OF TWENTE. | DIGITAL SOCIETY INSTITUTE

1 Abstract

The main focus of this research is to study and analyse catheters, which are instruments used in endovascular interventions. Starting from extensive research about the catheter specifications and material properties, these are required in order to create an accurate model of the catheter. Endovascular surgeries are used as a minimally intrusive method to diagnose or operate. The drawbacks are seen mostly in imaging used to see where the catheter is being pushed to and the main source of imaging is from CT scans, which causes radiation to the patient and the doctor. This radiation over years can be detrimental to the health of surgeons that perform a lot of these procedures. While the catheter is being used, there is force exerted on the vessels due to traversal of the catheters that can cause damage depending on how bad it is. Since this therapy depends heavily on haptic feedback and experience, a basic simulator which can be expanded is to be built along with force estimation and appropriate deformation.

For the purpose of building a simulation, the SOFA framework is used in order to model the catheter. This software is a physics based simulation software, which is mainly used in case of medical simulations which makes this an ideal tool for the research. Modelling on this software also provides us with contact forces and interactions with the vessel. The mesh will be design similar to a vessel except the mesh being rigid since it makes computations easier. The main goal is to design an accurate model of the catheter. The simulation is used to measure deformation and estimate contact forces which can be used to limit contact points and also help with optimal insertion minimizing force. A controller is also planned to be added as a means to navigate the catheter with haptic feedback to train with simulations and using the master manipulator part of the CathBot.

Contents

1 Abstract **2**

2 Introduction **5**
2.1 Clinical context . . . 5
2.2 Use of robotics and CathBot . . . 6
2.2.1 CathBot: An endovascular surgical Robot . . . 7
2.2.2 Haptic feedback: significance of feel . . . 7
2.3 Importance of Simulation . . . 8
2.4 Research objectives . . . 8

3 Background **9**
3.1 Robot assistance in endovascular intervention . . . 9
3.1.1 Steerable catheters . . . 9
3.1.2 Robotics used in assistance with procedures . . . 10
3.1.3 CorPath GRX Robotic System . . . 11
3.1.4 R-One robotic system - Robocath . . . 11
3.1.5 Hansen Medical - Sensei® Robotic Catheter System . . . 12
3.1.6 Hansen Medical - Magellan™ . . . 12
3.2 CathBot - An endovascular Robot . . . 14
3.2.1 Haptic feedback . . . 14
3.3 Simulation - SOFA Framework . . . 17
3.3.1 BeamAdapter Plugin . . . 18

4 Creation of simulation environment **19**
4.1 Using the SOFA Framework . . . 19
4.1.1 Modelling of catheter . . . 19
4.1.2 Simulation behaviour . . . 20
4.1.3 Constraint problem . . . 21
4.1.4 Contact detection . . . 22
4.1.5 Collision response . . . 23
4.1.6 Computation of forces . . . 24

5 Experimental evaluation **26**
5.1 Experimental setup . . . 26
5.1.1 Requirement : Catheter . . . 26
5.1.2 Requirement : Test mesh . . . 26
5.1.3 Requirement : ATI mini-40 force torque sensor . . . 27
5.1.4 Requirement : Mount . . . 28
5.1.5 Requirement : Actuator . . . 28
5.2 Simulation setting . . . 29
5.2.1 Evaluation procedure . . . 30

6 Results and comparisons **32**
6.1 Sensor output 32
6.1.1 Force plots 32
6.2 Simulation output 33
6.2.1 Force plots 35
6.3 Instrument deformation 41
6.3.1 Experimental deformation 41
6.3.2 Comparison and evaluation 43

7 User Interface **46**
7.1 Customization and simulation settings 46
7.1.1 CathBot integration 46
7.2 Graph tab 48
7.3 Forces tab 48
7.4 User Feedback 49

8 Discussion **51**

9 Conclusions **53**
9.1 Limitations and future work 53

10 Bibliography **55**

11 User manual **58**

2 Introduction

2.1 Clinical context

Catheterization[1] is the procedure of making a small incision in an artery or a vein in the arm, groin or neck in order to insert a small flexible tube known as a catheter to reach a target region where complications have occurred. The catheter is used to either diagnose or treat a condition with a minimally invasive approach. This method is used to treat and diagnose cardiovascular diseases[2]. It is the leading cause of death globally with an estimated number of 17.9 million deaths each year[2]. Open heart surgery is the treatment used to cure vascular diseases outside of these minimally invasive procedures. These surgeries have major risks and also cause very severe problems during recovery.

Use of catheters makes it easy for surgeons to access areas that are only possible otherwise by direct surgeries. Endovascular interventions have become more popular and widely used for treating cardiovascular diseases. Guidewires are used to traverse through the vasculature to reach the target to either diagnose or treat conditions without direct surgeries and the catheter helps in achieving this task with their flexibility and ability to reach secluded regions in the vasculature. They are very soft and also exert very little force on the tissues. Guidewires go through catheters and follow the shape to curve around vessels without damaging them.

The challenge with minimally invasive surgeries has been the requirement of experience and dexterity. Since navigating through vessels can be a challenge with minimal imaging, better treatment comes from better experience of the operator. Imaging mainly depended on X-rays and use of contrast agents, X-rays are a source of high radiation which is bad for the operator over the course of years and contrast agents being mildly toxic and used inside the patient to see the pathways more clearly. These are a few of the drawbacks of minimally invasive procedures. To tackle issues with experience and dexterity, robotics can be introduced with a lot of future implementations. With the risk of damaging vessels due to pressure while navigating with the hands, robotics offers the advantages with a more controlled approach with the help of feedback and more accurate movement. Using robotics, catheters and guidewires can be moved more accurately, making treatments a lot more effective and efficient while also being easy to recover from.

One of the main limitations of an endovascular intervention is an endoleak. This occurs during the procedure to treat aneurysms. Although these interventions are easy to recover from and temporarily fix an issue, there are after effects like an endoleak. An endoleak is a complication that occurs when the flowing blood leaks into the aneurysm between the gaps of the endovascular graft placed in order to fix the aneurysm. This is shown in the image 1. The graft basically replicates the shape of the normal vessel and reduces the swelling and reduces

the risk of internal bleeding. These endoleaks have different types which are categorized by how the endoleak is caused in the first place. In case of one of these occurrences, treatment has to be done again since an endoleak can cause bloating and rupture of the aneurysm.

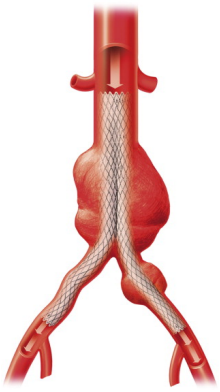

Figure 1: Endovascular graft in an aneurysm[3], placed in order to regulate blood flow; moved in with the help of guidewires/catheters

One of the other limitations of a minimally invasive procedure is that it has to be treated again in the near future and is not considered a permanent solution for the long-term. During the use of a catheter, if the forces exceed a certain amount when pushed against vessels, it can also cause rupture and internal bleeding. This is one of the main reasons why robotic assistance has been considered because of the accuracy of motion and lower force exertion.

2.2 Use of robotics and CathBot

Since minimally invasive techniques use the traversal of guidewires through the vasculature, use of robots can provide a more stable approach in terms of this application. Use of a robot typically just depends on the control of the guidewire insertion using a simple master-remote manipulator mechanism. There are robots available currently in the market for these surgeries, but each of these procedures are expensive and the robots are massive in size, making the installation and use complicated. The use of robotics in the medical field started around late 20th century. Robots used currently and previously in the endovascular field are discussed briefly. [4] The robots introduced for endovascular applications are listed:

- CardioARM
- Niobe
- Amigo
- Aeon Phocus

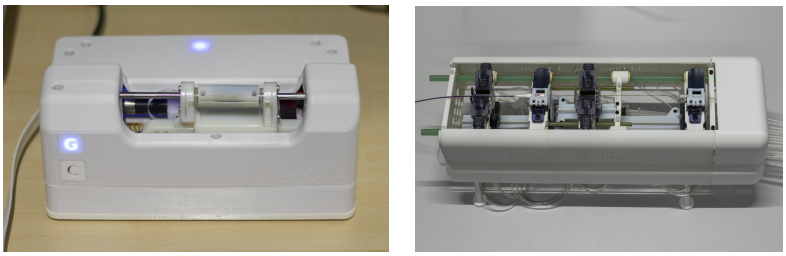

(a) CathBot master manipulator (b) CathBot remote manipulator

Figure 2: CathBot device setup

- CorPath GRX
- R-One
- Hansen Medical - Sensei® Robotic Catheter System
- Hansen Medical Magellan™

2.2.1 CathBot: An endovascular surgical Robot

CathBot is a simple master manipulator-remote manipulator robot which has options to operate both the catheter and the guidewire on the remote manipulator. This remote manipulator is able to push and pull the catheter and guidewire and also twist both of these depending on how the master manipulator is moved and rotated. The master and remote manipulator(shown in image 2) are integrated with simple RJ45(widely known as Ethernet) cables and the motors on the remote manipulator are powered with compressed air to move and rotate them. This is integrated with the help of ESP32(microcontroller) and is a very cheap and efficient setup. The bot in itself is also small and easy to move around and integrate since it doesn't require a lot of effort to install and operate.

2.2.2 Haptic feedback: significance of feel

Haptic feedback is useful and necessary when using a robot for endovascular applications, to navigate through the pathways since when there is a collision, there is no way of knowing without any sort of feedback. While performing a manual surgery, the feel of hitting walls is what helps surgeons navigate through more easily. The addition of haptic feedback with the bot will help in knowing where the catheter is and also how to proceed. There is an available system which relies on 3D vision[5] to provide haptic feedback on the end of the robot. This works with respect to the tip of the instrument and depending on the distance from the walls using imaging and a damping factor modelled in order to provide realistic feedback. The robot can be integrated with the software in

order to be used with the simulation to get a similar feel when used with phantoms and to also train on using the robot in real-world applications, bringing us to the research objective.

2.3 Importance of Simulation

In the case of a procedure using catheters, for the purpose of easier access, the traversal of the catheter must have limited contact points with the walls and also minimize force exerted. By having a simulation environment which allows access to use of catheters with different phantoms and estimating forces and behaviour of the catheter provides information without having to perform a practice procedure in a real environment. We try to estimate this performance with comparison of a catheter available in the lab. Being able to control this catheter in the simulation with the CathBot also gives experience with the robot and shows the feasibility and performance of the whole setup.

2.4 Research objectives

The availability of a variety of catheters helps reach secluded places where aneurysms or other issues might be located. Current day market offers thousands of different options depending on the target region. The modelling of a few specific catheters available at the lab and simulation of it in order to estimate forces and behaviour of the shape helps in knowing force exerted on the vessel like mesh to extend with providing haptic feedback on the master manipulator. The objectives of this research will be:

- To model catheters available in the lab in a simulation environment with mechanical properties and shape defined
- To estimate contact forces when traversing through a vessel like mesh and comparing with real-world experiment of the same
- To record deformation of the catheter while traversing through the mesh

Reduction of contact points during a procedure reduces any kind of damage on tissues, force estimation and motion of the catheter being estimated can help during procedure to minimize damage and also know the behaviour and risks. With the help of simulation environment, behaviour of the catheter can be approximately studied and trained on to help with experience and increase recovery rates. Robotic surgery is a long way from being realised properly and more data on catheters analyzed can help the field in the future.

3 Background

3.1 Robot assistance in endovascular intervention

In this section, the previously discussed technologies will be delved deeper into to see the current state of the field. Physics and robotics can be used in different ways to assist with surgical intervention. Primarily, there are two distinct ways that have been practised and have been useful in aiding with this goal.

3.1.1 Steerable catheters

Usually, catheters are used to reach different points in the anatomy. Different shapes are used so reaching more extended regions is easier. Instead of using different catheters, the idea is to make one catheter which is steerable in different directions. This technology is made possible by making the catheter actuate using magnetic field or activation. There are different types of active steerable catheters:

- Pull-wire mechanism
- Smart-material actuated
- Hydraulically driven

Pull-wire Catheter A catheter with a pull-wire mechanism to modify its shape is used in interventions to reach a larger anatomy. This works by use of flexible wires running inside the catheter that can change the configuration of the catheter because of attachment points on the tip or other parts of the catheter where the shape needs to be modified. These wires are attached to a pull-wire lumen which can be moved accordingly and the translation is shifted to the distal end. The image of this mechanism is shown in Figure 3

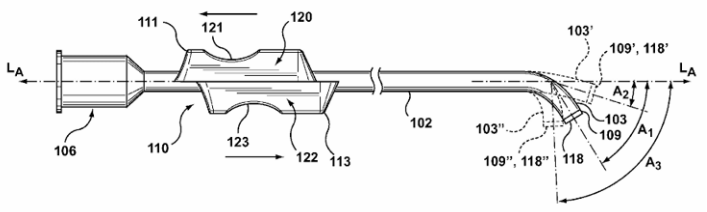

Figure 3: Detailed image of a pull-wire catheter

Smart-material actuated This depends on the material of the catheter which changes shape and responds to fields(eletric or magnetic depending on material) by changing orientation to reach different parts of the anatomy. There are a few different types of actuators available in this case. Shape Memory

Advantages	Disadvantages
Visualization of procedure with fluoroscopy	Long setup time
More degrees of freedom based on the robot	Expensive technology
Surgeon not exposed to radiation, remote surgery	Typically bulky, requires a lot of room
Easier to operate on	

Table 1: Surgical robotic system discussion[4]

Alloys(SMA) are known to be able to change shape and undergo significant deformation and return to their original shape upon heating. This is mainly of the material Nickel-Titanium[6], which can be used to get precise control over where it is navigated to. Other examples are magnetically actuated catheters and catheters with piezoelectric materials; magnetic actuation catheters[7] can be used non-invasively and are known to be used to treat clots in the body. These cannot be used with MRI which is a drawback; Catheters with piezoeletric materials change shape and create motion under the influence of an eletric field and are mainly used for drug delivery[7] in the body.

Hydraulically driven The hydraulic pressure drives these catheters through pistons to create a motion and modify the shape of the soft tip. The mechanism and the working is shown in Figure 4. In this reference, they use a bellows actuator with a single control tube. When the motor runs, the piston moves increasing pressure causing an inflow and making the bellows bent. The volume changes the movement of the bellows accordingly. This is paired with an optical sensor with a diode which converts light to voltage.

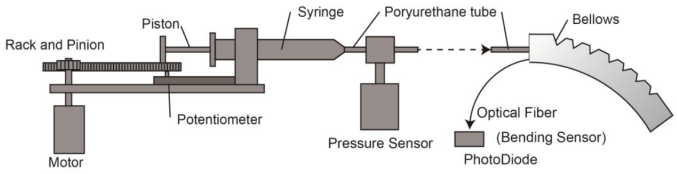

Figure 4: Hydraulically driven catheter setup[8]

3.1.2 Robotics used in assistance with procedures

In the previous subsection, mechanisms used to manipulate catheters were looked into. In this part, use of robotics in order to navigate and control available proprietary catheters are discussed more into detail. The table 1 discusses the advantages and disadvantages of the use of robotics in minimally invasive procedures by looking at the available robots in the market. In the following sections, only robots used in assisting with endovascular procedures are discussed about in detail excluding robots that solely provide imaging assistance in surgeries.

3.1.3 CorPath GRX Robotic System

Originally made by Corindus, acquired by Siemens Healthineers in Erlangen, Germany, this is a robotic system which is used to handle guidewires and catheters. The CorPath GRX translates movement in the controller to the end effector with precision and the movements are very minute to minimize risk. The system required to operate is a separate station making it radiation-free and also has a lot of additions for the hardware and software which include[9]:

- Fixates on placement of guidewire and the device when catheter is being moved by advancing or retrieving the guidewire to move relatively with the catheter to make sure there is no change in position with respect to the catheter; active device fixation[9]
- Very low and precise speed in order to reduce risk of damage, capped at a maximum of 6 mm/s[9]
- Possibility to accommodate microcatheters and microguidewires when required for neurosurgery
- Software improvements to accommodate extend working length in order to reach the target while using micro instruments

Figure 5: CorPath GRX robotic system arm and controller[10]

The controller and the arm are shown in the image 5 and these require a whole station to operate which includes the CT scan imaging integrated to it.

3.1.4 R-One robotic system - Robocath

Much like the system of CorPath GRX, this is an endovascular robotic system. It consists of a robotic arm that has a few tracks available for the placement of the instruments. One track is for the guidewire, one is for the stent/balloon[11].

There is a backup track that is used whenever another guidewire or another instrument is needed. This system can only be used with balloon catheters unlike the CorPath GRX. The movements are very precise with the controller being able to translate or rotate the arm and any track. Provided with a control station in order to control the arm from a radiation-shielded room. The imaging is linked with the station where you can control fluoroscopy and live images are also provided. The image of the system and the arm are shown in figure 6.

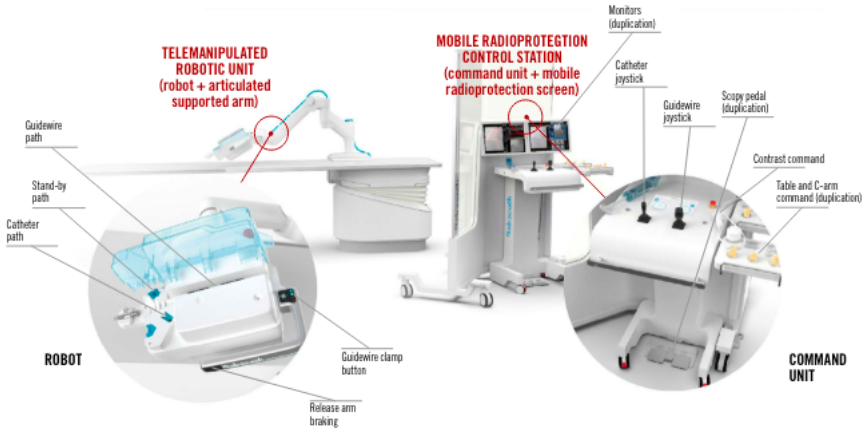

Figure 6: R-One Robotic system[11]

3.1.5 Hansen Medical - Sensei® Robotic Catheter System

This was a robot mainly designed to be an upgrade and also tackle a lot of previously faced adversaries. With the other robotic systems, the common theme of issues was that it was hard to reach a specific point without accurate hand to controller translation. The Sensei® was designed to provide motion translation in a stable and controlled manner. This project has been approved[12] by the Food and Drug Administration(FDA) in the US for unconditional Investigational Device Exemption(IDE)[12] and there have been multiple procedures that have used the Sensei® X for ablation procedures worldwide. The image of this robotic system is shown below in Figure 7. This robot also provides 3D visualization of the vasculature with the purpose of bringing more accurate procedures and visual aid for the clinicians. The Sensei® also provides forces acting on the catheter which can be felt as feedback while handling the arm to navigate through the vasculature.

3.1.6 Hansen Medical - Magellan™

Following the Sensei® X Robotic Catheter System, a system for endovascular interventions called the Magellan™was also designed. This was the first ever

Figure 7: Hansen Medical Sensei® X

robotic system for a vascular procedure. Using the architecture of Sensei® with the visualization, motion control and hand to catheter movement, the Magellan™specializes for endovascular interventions to assist vascular surgeons. The system allows you to steer the tip of the catheter corresponding to the motion of the controller making the movement through the trajectory way more stable. In the figure 8, the robotic arm is shown which is operated from a remote

Figure 8: Hansen Medical Magellan™[13]

area with the master manipulator.

3.2 CathBot - An endovascular Robot

CathBot is a simple master-remote manipulator robot which was introduced earlier in the previous section. The master manipulator of the CathBot is shown in figure 2a. As seen in the image, it has two buttons for two modes, one for using the catheter and one for using the guidewire. For each of these modes, different motors on the remote manipulator in figure 2b operate accordingly. There are two microcontroller modules which are used for the catheter motors and the guidewire motors. The setup is powered by air tubes and the motors operate on air. This is a robot that is very easy to install and very easy to move around. The master manipulator can be operated remotely from a radiation-shielded room with the remote manipulator operating through, moving the catheter and guidewire correspondingly. The architecture of the master manipulator[14] is shown in the figure 9. In order to understand how this functions with the remote manipulator, the architecture of the remote manipulator is also illustrated[14] in figure 10. The motion in the remote manipulator translate the motion from the master manipulator into micromovements so that the precision is higher and force exerted and contact points are reduced. This is also a very cheap design and easy to use making it very advantageous to use. The few drawbacks to the CathBot include its limited range which is stuck in the plane of the remote manipulator being able to only move within that plane. This is an ideal bot for being used in a situational manner to reach more secluded areas of the vasculature with precision and decreased risk of damaging vessels. The features of using CathBot include:

- Versatile device; MR-safe and also fluoroscopy compatible
- Multi-purpose; can be used for different types of interventions
- Extended access; rotation and translation of both instruments
- Very safe approach; the translation factor is very little to minimize contacts and force exerted
- Remote procedures; procedures can be done from a different room shielded from radiation

3.2.1 Haptic feedback

With the CathBot, whenever there is a collision with a wall, there is an increase in resistance while moving the linear controller and this helps with the advantage of being able to feel the region being navigated through. The movement of the master manipulator also depends on the remote manipulator's information which is sent back. This makes haptic feedback to an extent possible. Lack of feel usually makes decision making[15] very hard for the operator since this is one of the key aspects of an endovascular intervention. The availability of imaging is not enough since most systems only provide 2D imaging and the inability to see the other axis limits information on where the instrument is

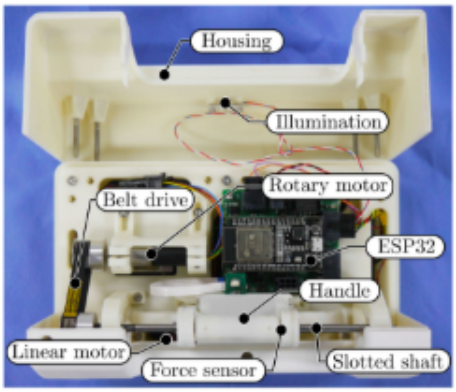

Figure 9: Master manipulator inner view[14]

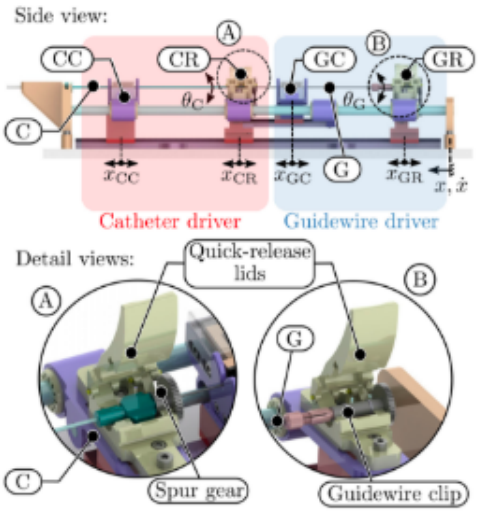

Figure 10: Remote manipulator components[14], C - Catheter, G - Guidewire, A - Actuation unit, CR - Catheter Rotation, GR - Guidewire Rotation, CC - Catheter Carrier, GC - Guidewire Carrier

being navigated through and also does not show collisions occurring in the third dimension. Currently, there are a few devices such as Sigma 7, Premium 3.0 master hand controller and HD2 which provide haptic guidance and have also been deployed in the teleoperation field[15][16]. As discussed earlier, haptic guidance has helped over the years without robots to be able to navigate through to the target while manually doing a minimally invasive procedure and the availability of this in any fashion would help in guiding the operator and making the procedure easier.

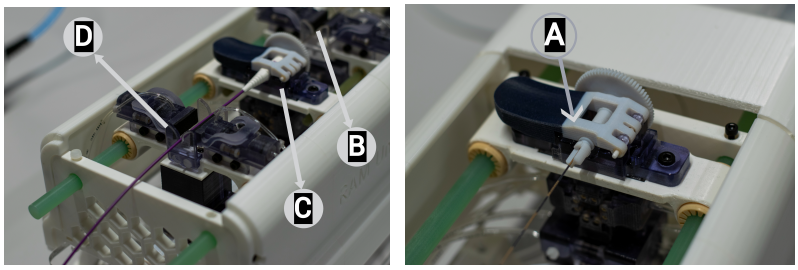

(a) (b)

Figure 11: Catheter Remote Manipulator where (a) shows B - Guidewire clamp, C - Catheter driver, D - Catheter Clamp and (b) shows A - Guidewire driver

3.3 Simulation - SOFA Framework

SOFA is an open-source simulation software mainly used for medical simulations. This software is coded mainly in C++ using object oriented programming to define all the elements. In SOFA, every element uses a multi-model representation[17]. The multi-model consists of specifically 3 models inside the simulation environment. For every body, we require these following three models, which are explained as:

- Behaviour model - The model of the body which defines the shape; the mesh of the shape and the size and similar aspects and what it is comprised of
- Collision model - The body made up of blocks of collision in order to simulate colliding with other bodies and corresponding response from the interaction
- Visual model - The visualization of the behavioural and collision model just to make the simulation more realistic in the way it looks

These models are all combined for every body and this is done by a feature called mapping. The object, collision model and visual model are mapped together using commands on the framework which combine these to integrate into the body which then looks, behaves and comprises of the features provided. A visual illustration of this is shown in the image 12. The approach to every

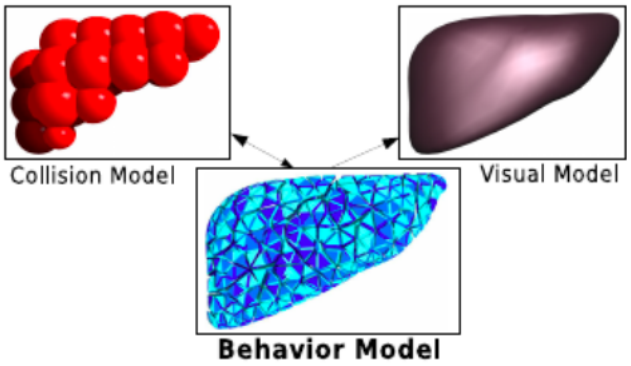

Figure 12: Multi-model representation of SOFA[17], where the collision model, the visual model and the behavioural model are all mapped together to make up the object in the environment

object and every interaction on SOFA is by using FEM. The Finite Element Method splits the whole body into smaller segments and smaller interactions. All these small interactions of all the smaller parts are combined to get the output of the whole body. The basic coding is done in an XML scene file which can be modified however the simulation needs it to be. The fundamental

requirements of every simulation starts from a AnimationLoop component. This is as the name says, the animation loop that keeps things running. This is followed up by the body's behavioural, collision and visual models. If there are multiple objects and interactions are meant to be seen, the soft objects require solvers that calculate the position and force values. Each scene also requires a collision response, collision pipeline and collision boundaries in order for these interactions to show. FEM Force fields can be used to visualise and apply forces on a body if required. Each scene also requires the mandatory plugins and optional plugins that are used for specific objects and interactions. We look mainly into the BeamAdapter plugin since it helps in modelling a beam-like object which is used as the catheter.

3.3.1 BeamAdapter Plugin

The BeamAdapter plugin is a component on SOFA that implements the available features on a 1-D scale. It uses FEM to construct beam-like structures which we can use to model a catheter or a guidewire which will be useful in medical simulations. The modelling is based on Kirchoff's Rod Theory and the plugin also offers deployment options for these beams. The beam-like structure is shown in figure 13. For collisions to take place and yield results, we require ConstraintSolver components which use the Jacobian matrix and Lagrangian multipliers in order to linearize the problem and map the physics to the constraints. This will be discussed about more in the next chapter.

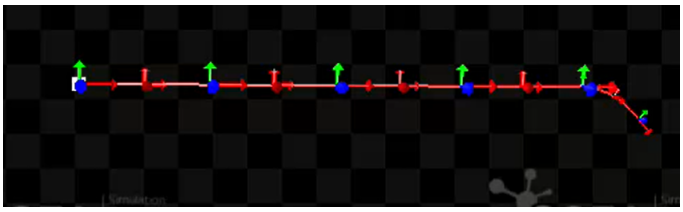

Figure 13: Beam designed on SOFA; shows multiple beams connected together to make up a bigger beam which has to compute interactions for every single beam; the X,Y,Z axis indication in green, blue and red is where every new beam starts

4 Creation of simulation environment

4.1 Using the SOFA Framework

The SOFA Framework introduced in the previous chapter is used here to create a simulation environment for an endovascular intervention. This includes creating and modelling the physical behaviour of endovascular catheters and target anatomy(here arteries) including their interactions in the form of collisions and contact forces. The developed simulation environment will then be assessed via simulation vs real-world experiments described in the following chapters.

4.1.1 Modelling of catheter

In order to realise a different tip shape on the simulation environment, a mesh of the tip shape has to be created. The BeamAdapter plugin offers an inbuilt function that has two sections called RodMeshSection and RodStraightSection. The straight section is the straight part of the catheter. We can replace the RodMeshSection with any mesh. Here, we require a mesh that traces the center line of the shape. To create this trace, a component called curve is used on Blender. This is a 2D curve which is used to fit the shape of the tip of the catheter. This is done by using the image from the website of Merit OEM as a reference in the background and tracing it along the tip shape. The scale of this catheter image is also changed in such a way that this size compared to the artery mesh we later use is the equivalent of the same comparison in the real-world.

For the purpose of simulation, we consider 2 catheters available at the lab. The names and the specifications are shown in the table below: These catheters

Model number	Tip type	Inner Diameter	Length	French-size
56535RIM	Rim	1.02 mm	65 cm	5F
565382CB2	Cobra 2	1.17 mm	65 cm	5F

Table 2: Catheter specifications[18][19]

are the products from Merit OEM. The properties of these catheters are used for simulation purposes and to model the behaviour as accurately as possible. For the shaft of the catheter, the material used is braided stainless steel as mentioned in the datasheet[20]. However, the coating on top of this is a hydrophilic coating used for every catheter. These coatings are typically polymers like polyethylene, PTFE etc. that are water-resistant. The mesh used for 565382CB2 and 56535RIM are shown in Blender in the image 14. This is given at the RodMeshSection and it only requires the center-trace of the shape in order to recreate it on SOFA. The first required parameter in the simulation environment is the Young's Modulus of the material. Both the mesh section and the tip section can be given different material properties since in SOFA, the

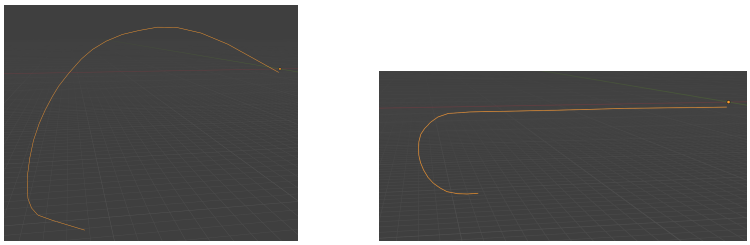

(a) 565382CB2(Cobra 2) (b) 56535RIM(Rim)

Figure 14: Blender meshes

RodMeshSection and the RodStraightSection are combined as the WireRestShape component which will be the shape of the whole catheter. When it comes to Merit OEM's catheters which are mainly used for endovascular applications, the mesh section which is basically the tip shape, is usually more resistant and more durable than the body. These materials could be a wide variety of alloys out of which we mainly consider polyurethane and PTFE and also the materials used in [21]. This source discusses about specific material catheters and their mechanical properties. These values are also given in the table 3.

Material	Young's Modulus
Silicone(used catheter)[21]	9.7 ± 0.4 MPa
Silicone(unused catheter)[21]	8.7 ± 0.5 MPa
Polyurethane(used)[21]	31.6 ± 0.5 MPa
Polyurethane(unused)[21]	44.3 ± 1.6 MPa
PVC(used)[21]	26.5 ± 0.8 MPa
PVC(unused)[21]	17.8 ± 1.2 MPa
PTFE[22]	0.392 - 2.25 GPa

Table 3: Table of materials

4.1.2 Simulation behaviour

After adding the mesh made on Blender using BeamAdapter to make up the WireRestShape component, we are able to see the shape and the ability to move this catheter in a desired direction with the InterventionalRadiologyController on SOFA. This can be seen in the image 15. The InterventionalRadiologyController is a component that is a part of the BeamAdapter plugin that allows the user to steer a wire made on SOFA in a direction at a specific speed and the starting coordinates of the instrument have to be provided from where it is steered. This component also allows the user to be able to rotate the instrument.
Following the simulation environment, the interactions between objects and appropriate responses are given by a few different components on SOFA. As dis-

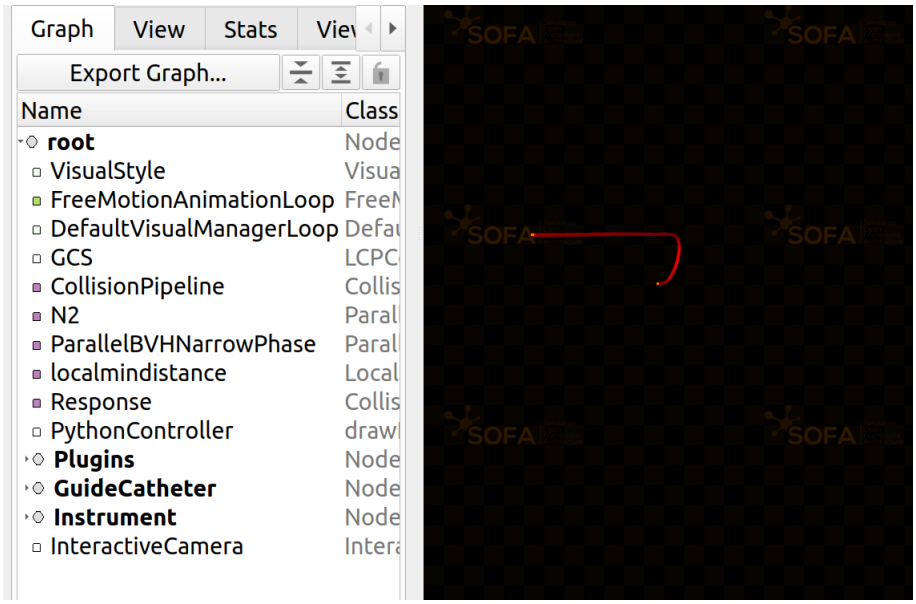

Figure 15: 56535RIM on SOFA

cussed previously, every simulation needs an animation loop along with collision models linked to the objects and appropriate responses in order to generate an interactive environment. The use of mathematical solvers aid in numbers which help us evaluate the simulation as a whole. While each solver gives out values, we specifically use a linear constraint solver called the LCPConstraintSolver which considers the constraints of the objects involved as their own mechanical boundaries beyond which collision occurs and results in interaction. This constraint problem is solved in a very specific way with this framework.

4.1.3 Constraint problem

The simulation system is considered a linear system which poses the well known F = ma using system variables. This system uses Lagrange multipliers which gives us the vector of the constraint forces where the multipliers are the forces in the local body frame. The dynamics of a body are defined by the equation[23]:

$$\mathbf{M(x)\ddot{x} = F(t) - f(x,\dot{x}) + W(x,\dot{x})} \tag{1}$$

This equation represents any moving object in the framework and the parameters in this equation signify the physics of the body. Starting off, M(x) is the inertial matrix of the body and x, $\dot{x}$ and $\ddot{x}$ are respectively the position, velocity and acceleration of the object[23]. Following this comes the forces and the constraints where F(t) is the sum of external forces on the body and f(x,$\dot{x}$)[23] is the sum of internal forces on the body. The last bit which is W(x,$\dot{x}$) is the factor that contains the boundary conditions of the body[23].

The simulation uses timesteps to simulate each instant of the scene. This is defined by the term dt which is a small change in time. Integration is used based on this time step in order to solve the differential equations and here, we used Backward Euler method implemented by the EulerImplicitSolver to solve motion values such as acceleration in order to move objects. While using Backward Euler formulation, the assumption of a differential is made such that(A simple equation of velocity is used for example):

$$\begin{aligned} \frac{dy(t)}{dt} &= \frac{y_n - y_{n-1}}{\Delta t} \\ \frac{y_n - y_{n-1}}{\Delta t} &= f(y_n, t_n) \\ \implies \frac{y_{n+1} - y_n}{\Delta t} &= f(y_{n+1}, t_{n+1}) \\ \implies y_{n+1} &= y_n + \Delta t * f(y_{n+1}, t_{n+1}) \end{aligned} \tag{2}$$

This means the information of a new time-step is calculated depending on this new time-step itself. The velocity update and position update are expressed as:

$$\begin{aligned} \Delta x &= x(t + dt) - x(t) \\ \Delta v &= v(t + dt) - v(t) \end{aligned} \tag{3}$$

Following Taylor-Series expansion of all the non-linear terms[23] and then adding it on to Equation 1, we get velocity update as:

$$\begin{gathered} (M + dt\frac{df}{dv} + dt^2\frac{df}{dx})\Delta v = -dt(f + dt\frac{df}{dx}v - J^T\lambda) \\ \text{This can be rewritten as :} \\ A\Delta v = b + dtJ^T\lambda \end{gathered} \tag{4}$$

Where J is the Jacobian containing the constraint directions[24] and λ is the set of Lagrange-multipliers which are computed by the ConstraintSolver.

4.1.4 Contact detection

On the simulation environment, without using components to detect contact between two behavioural models, they will pass through each other without any interaction. When two objects are in the proximity of each other, an algorithm is required to detect this occurrence and communicate with the software that there has been a collision detected. SOFA provides multiple options to do this and cause create contact. The method used is called LocalMinDistance[24] which is a built-in method of the framework. In order to optimize the contact points, this algorithm uses cones, which are basically combinations of orthogonal planes of neighbouring lines or surfaces in the body[24]. This idea is explained better with the help of illustrations in image 16. The gray regions are the cones which were explained about earlier, which are used to detect contact depending on the

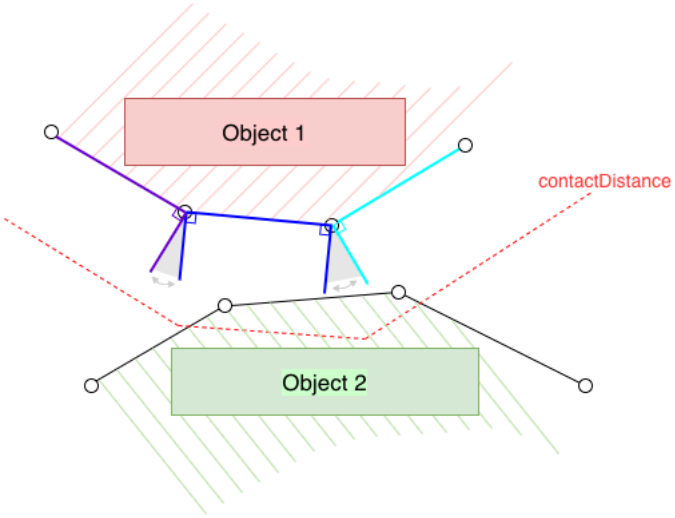

Figure 16: LocalMinDistance working[24]

contactDistance component seen in the image 16.
The LocalMinDistance has the components alarmDistance and contactDistance where contactDistance mostly matters since the former is only used as a benchmark to create contact as it is the maximum distance for which there is contact between the two objects. The contactDistance component is the distance beyond which there will be collision and appropriate response comes in. As seen in the image 16, the second object has passed the contactDistance and in this case, there will be contact and it will be with the geometrically closest point on the other object.

4.1.5 Collision response

This is the last part of the pipeline where after contact is detected, there has to be appropriate response. The response depends on whether the objects in the simulation that come into contact both move or if one of them is stationary. In this case, since the mesh is stationary, the contact created causes constraints at certain points in the MechanicalObject component which will serve as the object in the collision model linked to the behavioural model. Since ultimately, the collision model generates contact and responses, this is where the collision response is sent to. In this case, we use FrictionContactConstraint which is a simple response provided by SOFA and as the name suggests, acts as a friction response when the two objects collide and this constraint is solved by the ConstraintSolver in order to generate constraint forces which serve in calculating the contact forces.

4.1.6 Computation of forces

In order to find out what the contact and collision caused on the body with respect to force acting on the body, we need to go back to Equation 4, which contains the equation containing contact forces. The element $dtJ^T\lambda$ is available for every object containing collision models. These collision models contain the Jacobian which is computed based on contacts and collisions. This contains the constraint directions and this needs to be multiplied with values λ which is computed in a solver. Every solver in SOFA uses the Gauss-Seidel algorithm to solve constraint equations and calculate the Lagrange multipliers. The corresponding constraint needs to multiplied with the corresponding multiplier. These are done for every constraint and added up together. Every Lagrange multiplier is also multiplied with the time-step dt when we get it from the solver, hence we also need to divide this value by dt since the term $J^T\lambda$ is the constraint force acting on the body. To explain better, consider there is are 10 constraints on an object. For each of these 10 constraints, the solver computes Lagrangian multipliers giving us 10 values which are the forces directly normal to the body in the local frame of the body. This is repeatedly done at each time-step and the values get updated with every step. The example can be defined by the equation:

$$
\begin{aligned}
F_x(\text{caused by constraint 1}) &= \frac{\lambda(1)}{dt} * J_{01}(\text{Jacobian for the 1st constraint}) \\
F_y(\text{caused by constraint 1}) &= \frac{\lambda(1)}{dt} * J_{02}(\text{Jacobian for the 1st constraint}) \\
F_z(\text{caused by constraint 1}) &= \frac{\lambda(1)}{dt} * J_{03}(\text{Jacobian for the 1st constraint}) \\
&\text{01, 02 and 03 signifying the 3 elements in the Jacobian} \\
&\quad \text{being X, Y and Z conversions correspondingly}
\end{aligned}
\tag{5}
$$

For each of these constraints, in case there is a contact force, the Jacobian matrix of the object will contain values for that constraint, therefore giving us 10 matrices in case all of these said 10 constraints create a force. The Jacobian matrix of the object contains the conversion to X, Y and Z direction to the global frame for each constraint. These two are multiplied together for each constraint in order to convert the forces from local to global frame. As soon as this is done, we have the force caused by one constraint on the body. This is done for each and every constraint and added together at every time-step in X, Y and Z directions.

The image 17 illustrates better on why the conversion from local to global frame is required. The localized variables like velocity and displacement will be different compared to the same in the global environment. When the force is measured in real-world, local variables do not give us the full picture and the force that can be measured is always in the global frame with respect to us.
For example, the displacement u as you see, is the displacement in the global

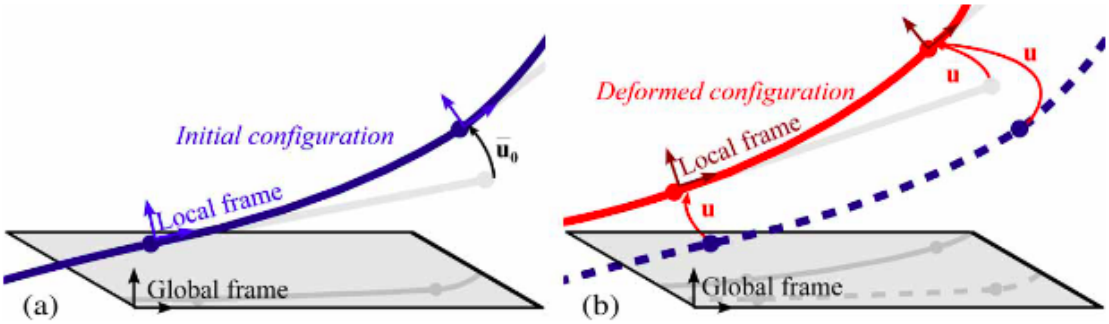

Figure 17: (a) Initial configuration of the beam in the local frame (b) Shows the deformed configuration in both the global and local frame[25]

frame. By assuming u' as the displacement in the local frame, the change in displacement from u_0' to u' can be related to the global frame displacement by the equation[25]:

$$u' - u'_0 = \Lambda u \tag{6}$$

Where Λ is the rotation matrix that converts the global frame displacement u to local frame u' - u'_0. The work done will be the same in both frames, and therefore we know that[25]:

$$\begin{gathered} \Delta u' f' - \Delta u f = 0 \\ \Delta u^T (\Lambda^T f' - f) = 0 \\ f' = K'_e \Lambda u \text{ (Where K'}_e \text{ is the stiffness matrix in the local frame)} \\ f = (\Lambda^T K'_e \Lambda) u \\ K* = (\Lambda^T K'_e \Lambda) \end{gathered} \tag{7}$$

This is the force displacement equation in the global frame, which is similar to what we use in order to calculate forces on SOFA in the equation 5.

5 Experimental evaluation

To assess the modelling of the catheter being consistent with the actual catheter, there has to be an experimental evaluation. The main metric used to evaluate the model is the force exerted by the catheter while conducting an endovascular intervention with a test artery mesh. This will be discussed about in detail along with other metrics in the next chapter. Following the simulation setup, this has to be repeated in real-world, therefore the required materials are discussed.

5.1 Experimental setup

The necessities for a setup in real-world to be able to test the models, the requirements are a catheter, a test mesh, a sensor to record forces on the test mesh and a stand that holds the test mesh along with the sensor.

5.1.1 Requirement : Catheter

For the purpose of the research and testing, some requirements were established. Since the objective of the simulation is to test the behaviour of catheters, a specific catheter which was available was chosen. The specifications of this catheter are shown in table 4. The 56535RIM[18] is also shown in the image 18. Following the catheter, we also require a phantom/mesh to test this catheter with in order to measure forces applied by the catheter. When it comes to

Model number	Tip type	Inner Diameter	Length	French-size
56535RIM	Rim	1.02 mm	65 cm	5F

Table 4: 56535RIM specifications[18]

material properties, the catheter is split into two parts. The tip is made of stainless steel coated with a hydrophilic coating, which we assume to be around 1-50 MPa as seen in table 3 and different trials are conducted to see the difference in values. The body of the catheter is assumed to be around 1-30 MPa since the ranges are so varying and it does not retain its shape as well as the tip does.

Figure 18: 56535RIM Merit OEM[[18]

5.1.2 Requirement : Test mesh

Using the 3D printing facilities available at the University of Twente, a simple solid artery with one entry and two exits is made and printed. This is also

available as a mesh on SOFA as a simulation object in order to make it as close to real-world as possible. The material used for this mesh is the clear resin from Formlabs. This is done in order to be able to see through it while moving the catheter through it. The test mesh in real-world has a structure on the bottom side in order to fit the Force-Torque sensor for the measurement of forces in X, Y and Z. The orifice has a diameter of 10 mm as compared to the catheter which is 1.65 mm. The mesh in real-world 19a and on Blender 19b are shown in figure 19. The vascular mesh in 19a is mainly used to record deformation and in order to create more contacts to measure significant forces, another mesh with a smaller diameter resembling a vascular phantom as well is used instead, shown in Figure **??** in both real-world and simulation environment.

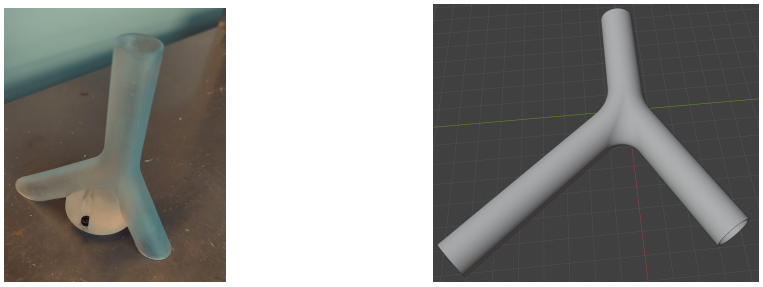

(a) Test mesh 3D printed at the lab

(b) Test mesh on Blender

Figure 19: Mesh comparison

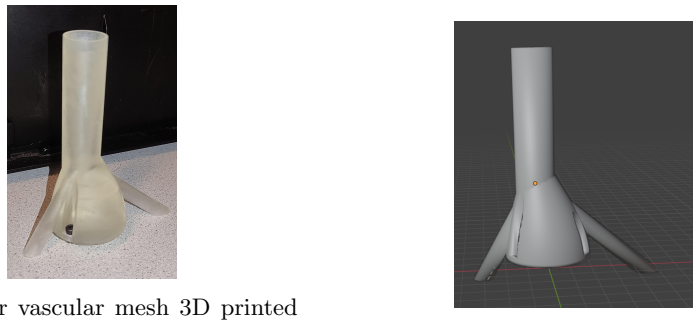

(a) Smaller vascular mesh 3D printed at the lab

(b) Smaller vascular mesh on Blender

Figure 20: Smaller artery phantom in real-world vs simulation

5.1.3 Requirement : ATI mini-40 force torque sensor

ATI mini-40[26] force torque sensor is used to measure forces in X, Y and Z axes and can also be used to measure torques in all 3 axes. The specifications of this sensor are given in table 5[26]. The time sampling factor is 1000 and counts per unit force is 100000 for the recorded results from this sensor.

Calibration	$\mathbf{F}_x$,$\mathbf{F}_y$	$\mathbf{F}_z$	$\mathbf{F}_x$,$\mathbf{F}_y$	$\mathbf{F}_z$
SI-80-4	80 N	240 N	1/50 N	1/25 N
	Sensing range		Resolution	

Table 5: ATI mini-40 Sensor specifications[26], where SI-80-4 is a variation of the sensor being the sensing ranges for Forces and Torques in X and Y axis, being 80 N and 4 Nm here

5.1.4 Requirement : Mount

The mount used for the setup including the mesh and sensor was also 3D printed and assembled together. This can adjust the height of the mesh for insertion which can be kept at the height of the robot in case of using the CathBot. The image of this mount is shown in figure 21.

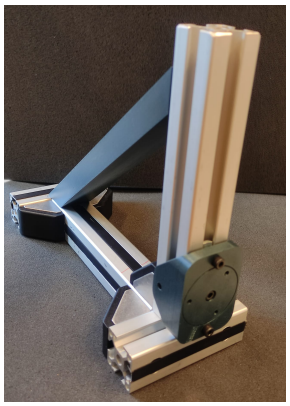

Figure 21: Mount for the mesh

To measure forces acting on the mesh, the bottom of the mesh is attached with the Force-Torque sensor which is then connected to a computer which can read the forces acting on the sensor. Since this is connected to the mesh, the force acting on the body will be recorded on the computer. With the insertion point being the side of the mesh with one entrance, there are two exits with most of the force coming from when navigating through the intersection point where the branch splits into two exits since there is friction while pushing against the walls.

5.1.5 Requirement : Actuator

To move the catheter in a straight line at a constant speed, we require actuation. For this purpose, an actuator from Actuonix is used. The model used here is Actuonix L16-140-150-6-R which extends in a straight line to 140 mm. Since

the phantom used is 98 mm, the whole distance can be covered at a constant speed. The image is shown in 22. The catheter is tied to the tip of this actuator

Figure 22: Actuonix L16-140-150-6-R

and it extends this catheter in a straight line into the phantom used in order to replicate what is done in the simulation.

5.2 Simulation setting

After discussing the fundamentals of the simulation software we use which is SOFA, the insertion procedure on the software needs to be as close to the setup as possible. The insertion into the mesh is done at a constant speed in order to match the same pace of the experiment. For comparison purposes, we set a test that has a length of 6000 time steps. Each time step is considered to be 0.001 seconds hence making it a test done in 6 seconds in real-world.

The catheter is modelled based on the BeamAdapter plugin as explained earlier in the section 3.3.1. Since this uses 1-D FEM, our catheter behaves like a 1-D beam which deflects and deforms based on the material properties given to it. Like discussed earlier, the Young's Modulus is assumed to be 1-50 MPa for the tip of the catheter and the proximal section is considered to be around 1-30 MPa. The radius of the beam is required to be set which is measured to be 0.825 mm since the inner diameter of the instrument from table 2 is known to be 1.02 mm which gives the radius of 0.51 mm.

Since the length of the whole catheter is 65 cm, the simulation constructs the 1-D beam with the help of smaller beam elements that make up the whole shape. Therefore, the more elements used, the more accurate the shape is represented in the scene. Since the length is known to be 65 cm, the number of beam elements chosen are 650, which means that the catheter is made up of 650 small beams that each have their own beam equations. This is done since the units used in the simulation were discussed earlier and we use millimeters for the length measure and 650 units would represent the 65 cm more or less ideally. The values in the table 6 compare the values used in the simulation and the available values. The thickness of the catheter is assumed to be 0.02 mm since it is very small and since we use millimeter as the unit of measurement, this difference is approximated and added in the simulation. The Young's Modulus of the tip is known to be around 1-50 MPa since the coatings are known to be soft and to make the instrument minimally invasive along with the proximal part of

		Catheter simulated
Parameters	**Catheter(real-world)**	**Trial 1**
Length(in mm)	650	650
Number of beams	N/A	650
Inner diameter(in mm)	1.02	1.02
Total diameter(in mm)	$\sim$ 1.65	1.65
Young's Modulus(GPa - tip)	1-50(assumed)	50
Young's Modulus(GPa - proximal)	$\sim$ 1-30(assumed)	26
Weight of the object(grams)	0.35	0.35
Mass Density(g/mm^3)	$\sim$ 0.007267	0.006729

Table 6: Simulation specifications

the catheter having an elastic modulus of around 1-30 MPa as discussed earlier. There might be a discrepancy in the value of the Mass Density, but because of this value being so small and the unit of weight used in the simulation being kilograms, this value goes down by another 10^{-3}. The approximation is done by considering the fact that the hub of the catheter weighs majority of the part. This change in Mass Density does not change the performance or the results.

5.2.1 Evaluation procedure

To test the models of the catheters in simulation and real-world, the exact same setups are used in both instances. The main metric chosen to compare these models is the force exerted by the catheter on the mesh. This is done to see how much force is actually exerted on the body as the primary goal is to reduce contact points and also the force exerted on the walls of the vessels. Following the force measurement, the deformation of the body is also measured with the help of a camera using the setup. With respect to SOFA, the image can be captured with the help of a screenshot from the top view. The difference in recordings is that the simulation outputs forces on the catheter since we take the Jacobians from the catheter's collision models while the forces recorded in real-world is the force acting on the mesh. The methodology of evaluation is discussed below.

Data sampling When it comes to values recorded, the time and forces have a sampling rate. Starting off with the Force-Torque sensor, the sampling rate of

the time is 1000 units, making each sample 0.001 seconds. This sensor also has counts per unit for of 100000 requiring us to divide the force values extracted by 100000 to get the actual value. These were discussed earlier in the same chapter. The same applies to the simulation except the force calculation was discussed in equation 5 and when it comes to handling, it was mentioned earlier that it is also 0.001s making the sampling rate 1000. In order to match the result graphs with time, both simulation and the experiment are recorded and the first 6 seconds are taken for both since it roughly takes about 5 seconds to traverse through the mesh on each trial.

Force processing For the experiment, there are 15 trials taken which are all processed in Jupyter notebook using Python packages pandas. The same is done with the simulation data and both of them are processed for 6000 samples. For the 15 samples, the mean from the 15 trials in each axis is taken and plotted. This in return is compared with the simulation data since there will not be any change with the simulation because mechanical values have to be changed in order to notice any difference. Using the mean values, the error rate is also plotted in order to notice the difference and the 15 trials are also used to calculate the standard deviation in order to see how much each trial deviates from the other trials.

Deformation of instrument The catheter while traversing through the artery undergoes contacts and deflections. The behaviour of the modelled catheter is compared to the real-life model by comparing the final configurations of different trials with the simulation configuration. The tip of the catheter in both simulation and the experiment are compared and the configurations are compared. The error in tip position is calculated and an Root Mean Square Error(RMSE) is computed by combining the error values in all trials.

6 Results and comparisons

From the setup of the experiment, we are able to extract forces with the help of the ATI Mini-40 Force Torque sensor. The orientations of the axes are described easier with the help of an image. When compared to the simulation, the natural axis along which we insert the catheter is defined as the positive X axis. Upwards orthogonally to X is considered as +Y axis and outwards is considered as +Z axis. This is the same orientation on SOFA and when it comes to the sensor, the whole system is different. To make things easier to understand, we stick to the conventional system used in SOFA. The +Z axis of the sensor is equivalent to -X axis in the simulation. The +X axis of the sensor is equivalent to the +Y axis on SOFA. By the right hand rule, we get that the +Y axis of the sensor is equivalent to the -Z axis of the simulation. To make things more understandable, look at table 7 and image 23.

SOFA Axis	**ATI Mini-40 Axis**
+X and -X	-Z and +Z
+Y and -Y	+X and -Y
+Z and -Z	-Y and +Y

Table 7: Orientation table

6.1 Sensor output

To record sensor values, the software provided by ATI is required. This software provides Forces and Torques on the three axes of the load cell. The recordings usually have a bias factor which includes gravity and air resistance and this can be removed on the software to measure the raw contact forces. The load cell data is logged in a text file which is processed on Python to analyze the data.

6.1.1 Force plots

For analysis, 31 trials were recorded in a similar manner by pushing the catheter straight into the vascular phantom. In every one of these trials, the catheter deflected towards the same exit therefore making our trials more consistent. The results from a random trial are shown in image 24. This phantom gets smaller from a diameter of 10mm to 6mm gradually and this creates way more contacts since it becomes smaller than the catheter size. Whenever the catheter traverses through the phantom, it gets gradually smaller and the catheter gets squeezed and causing forces on the walls and due to this, we are able to notice a spike in force up to 0.474 N and this is mainly seen in the negative X axis. When it comes to the Y and Z axis, the forces are almost zero being very low with Y axis having a spike of 0.0233 N and Z axis having a spike of around 0.0209 N. When the walls get smaller, there are way more contacts in the direction of

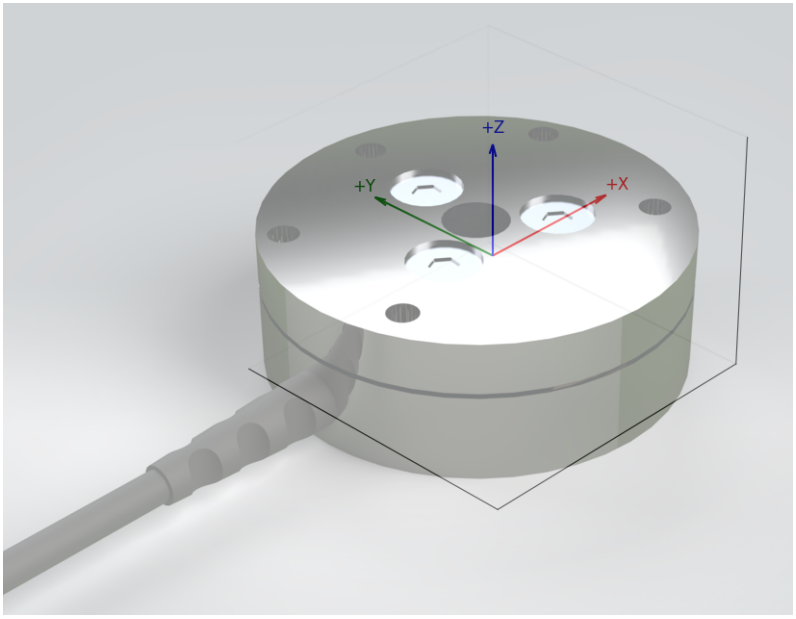

Figure 23: Orientation in real-world: Z-axis is in and out of the sensor, where the artery is connected making it in and out of the artery, Y-axis will be to the left and right of the artery where the branches are and X-axis is up and down

pushing and therefore, a lot of force is caused in the X-axis. The pushing seems evident whenever we see spiking in the negative X axis which shows fact that the walls are being pushed against.

By making the data more generalized by taking the mean of all the trials at every value in corresponding axes, we are able to plot the mean values from the 31 trials at each time sample. This can be seen in the figure 24.
From these set of graphs, the peaking in the X axis is seen around 4400 milliseconds which goes up to -0.473 N. This also explains the pushing of the catheter against the walls. The peaking in Y and Z are pretty negligible following a similar pattern from before. The advantage of using the mean of each trial also helps in reducing the noise from the sensor making it a more stable curve, this can be seen in 25.

6.2 Simulation output

The values calculated in the simulation using the formula in equation 5 is exported to a text file using a Python script for processing and analysis. The forces are calculated at the end of every timestep on SOFA using the force equation 5.

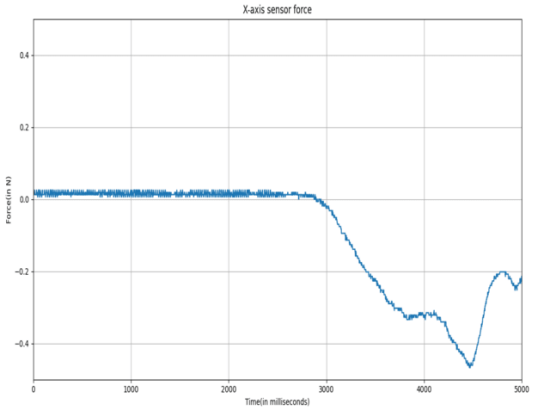

(a)

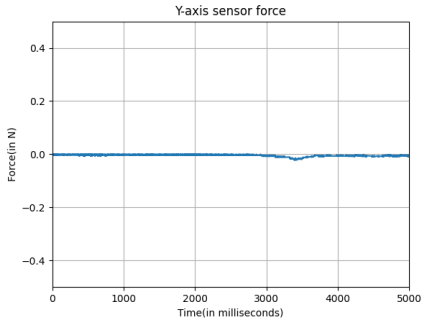

(b)

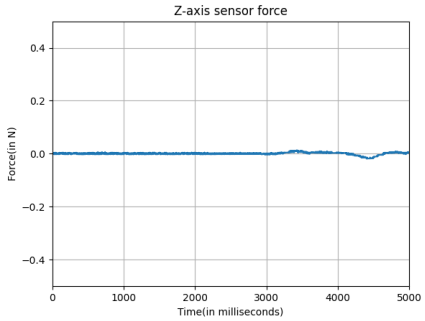

(c)

Figure 24: Contact forces measured by the Force-Torque sensor in (a)X-axis (b) Y-axis (c) Z-axis

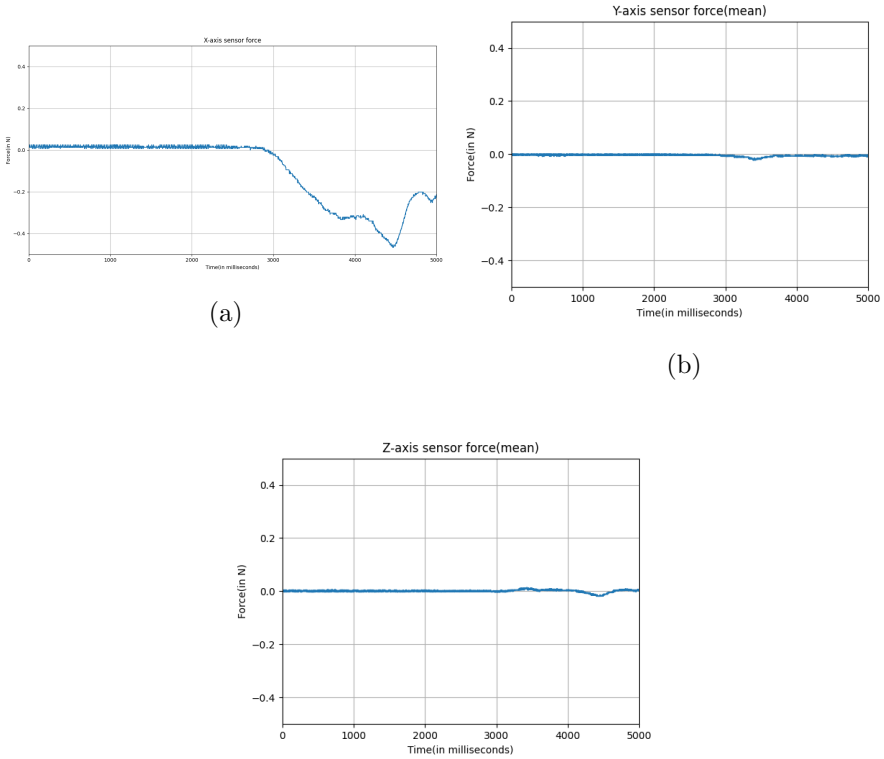

(a)

(b)

(c)

Figure 25: Mean of force sensor recordings in (a) X-axis (b) Y-axis (c) Z-axis

6.2.1 Force plots

The force plots on SOFA do not change with different simulations since it mainly depends on the parameters used and we use different parameters with each trial. For the purpose of testing, different parameters are tried for the tip and the proximal part of the catheter. These trials and parameters are specified in table 8. The graphs plotted for sensor forces in X, Y and Z axis are plotted against the simulation forces with the parameters in Trial 0, which are shown in the figure 26.

In the X-axis, the most force is seen in both simulation and sensor readings. These trials are simulated to be identical to the experiment done with the vascular phantom and in both of them, around 3 seconds is when the catheter enters the cagey part of the phantom where the diameter gets smaller than the size of the catheter and contacts start popping up. The peak with the parameters used in Trial 0 goes up to 0.598 making it almost 0.6 in the negative X axis. The values in Y and Z are very very low and almost negligible being around 0.050

	Parameters	
Trials	**Young's Modulus Tip(MPa)**	**Young's Modulus Proximal(MPa)**
Trial 0	50	26
Trial 1	40	26
Trial 2	37.5	26
Trial 3	35	26
Trial 4	30	26
Trial 5	40	15

Table 8: Simulation trial specifications

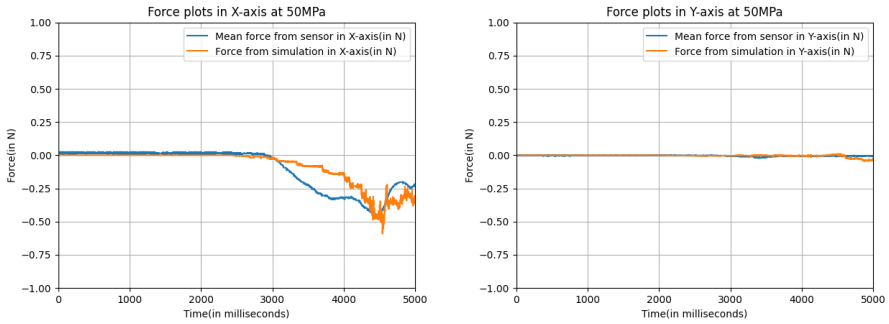

(a) (b)

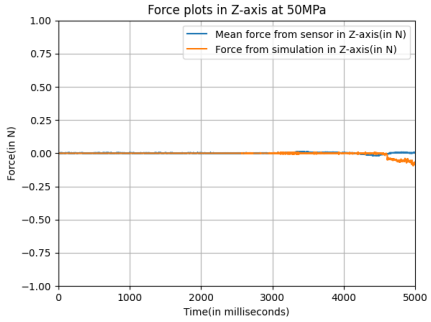

(c)

Figure 26: Shows simulation readings(orange) vs mean sensor readings(blue) in (a) X-axis (b) Y-axis (c) Z-axis

in the negative Y axis and in the Z axis around -0.1 N towards the very end of the trial. The following graphs will be of the next trials following in the order. The forces as seen in image 27 are very negligible in both Y and Z axes in every

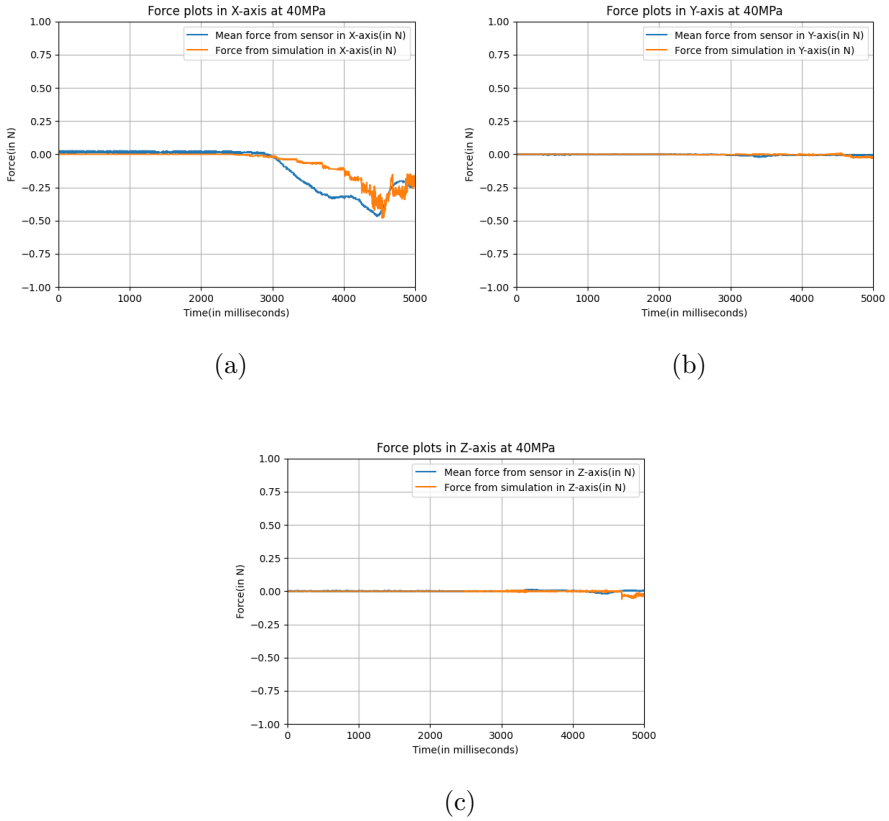

Figure 27: Shows simulation readings(orange) vs mean sensor readings(blue) in (a) X-axis (b) Y-axis (c) Z-axis

scenario and therefore, only X-axis force will be studied since these forces do not affect anything and the model also predicts negligible forces. In X-axis however, the peaking is around -0.497 N which is very close to the forces measured in the sensor. For the following plots, only the X-axis plots will be studied. From image 28, it can be noticed that as the Young's Modulus of the tip goes down, the forces also go down. The closest values to the peaking are from 37.5MPa, 35MPa and the last trial where the tip is 40MPa and the proximal part is modified for the first time to have a elastic modulus of 15MPa. These plots can be evaluated better with the help of error measurement. For this purpose, a mean of the absolute error and the root mean square error(RMSE) are taken for each of these trials in the X-axis and plotted. In order to get a measure of how low these values are in the Y and Z axes, the first plots will show these values for

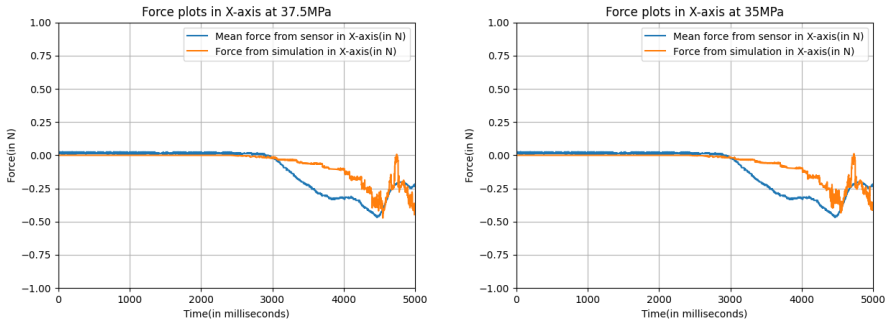

(a)

(b)

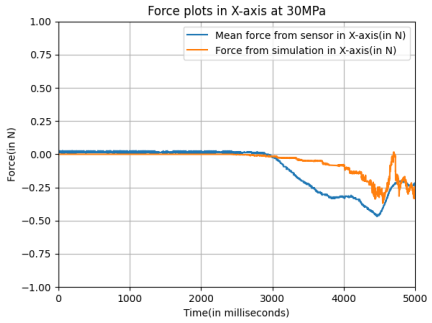

(c)

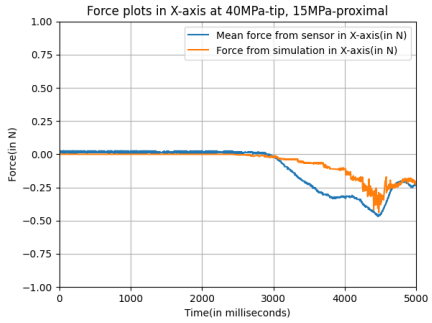

(d)

Figure 28: Shows simulation readings(orange) vs mean sensor readings(blue) in X-axis from (a) Trial 2(37.5MPa) (b) Trial 3(35MPa)(c) Trial 4(30MPa) (d) Trial 5(40MPa-tip, 15MPa-proximal)

the Trial 0 in figure 29.

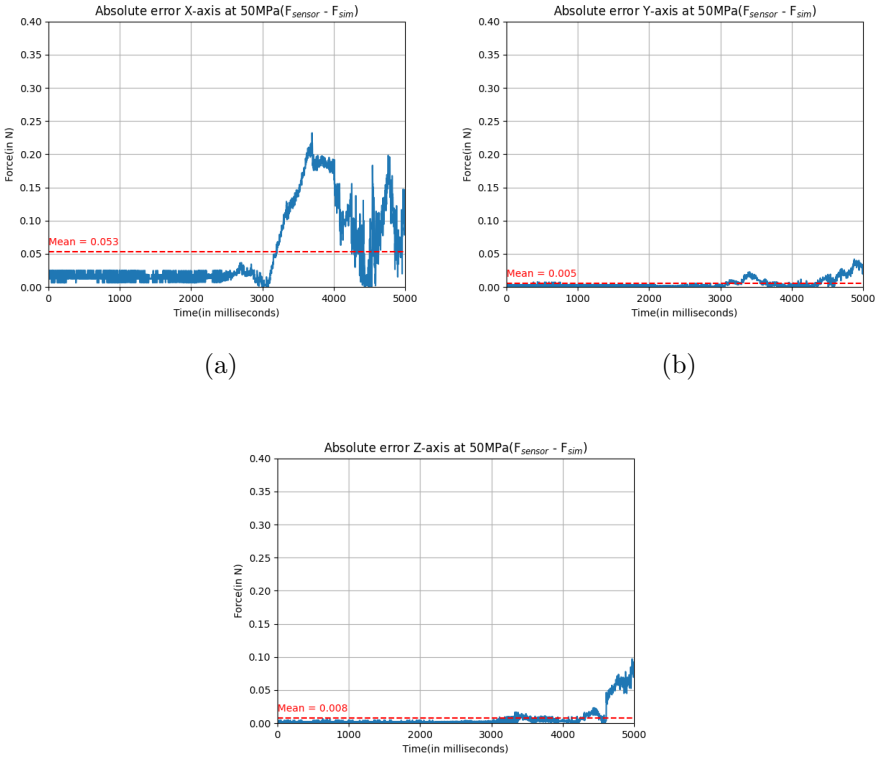

Figure 29: Shows absolute error values along with the mean error in (a) X-axis (b) Y-axis (c) Z-axis

The most error seen is in the X-axis since that is where there is significant force due to the interactions. The mean force over the 5000 milliseconds is 0.053 N in the X-axis. The mean in both Y-axis and Z-axis for Trial 0 are nearly 0 being around 0.005 N and 0.008 N respectively. As the values change and in this case, goes down, the error seems to increase since the catheter seems to be somewhere around 50 MPa for its material property. These plots show a peak error of nearly 0.25 N which is seen when the simulation is starting to detect contacts and in the experiment, the actuator pushes it against the phantom making it create more contacts and more force whereas in the simulation, it traverses through, facilitating in the mesh and slowly reaching the point where there's most contacts. This is why we see a discrepancy in force values even though the simulation predicts better with more contacts. Table **??** shows more details about the mean error and RMSE of each trial throughout the simulation

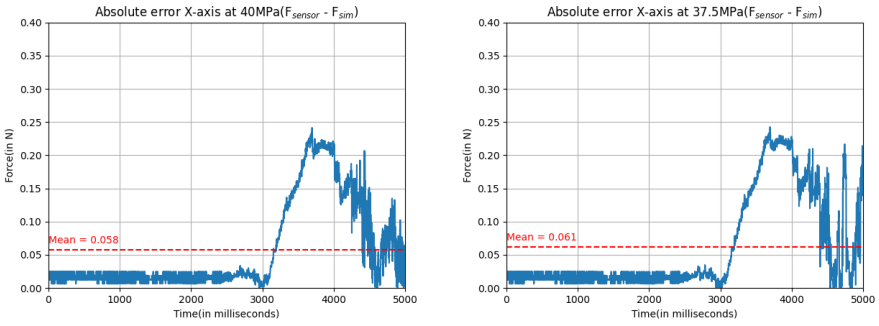

(a) (b)

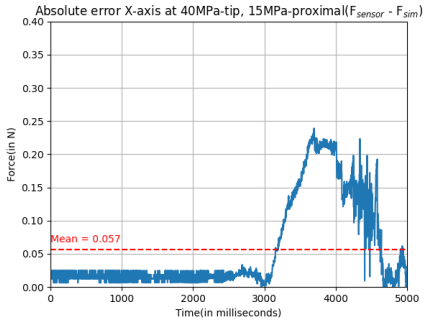

(c)

Figure 30: Shows absolute error values along with the mean error in X-axis from (a) Trial 1(40MPa) (b) Trial 2(37.5MPa) (c) Trial 5(40MPa-tip, 15MPa-proximal)

in all axes.

$$\text{RMSE} = \sqrt{\frac{\sum_{i=0}^{8} ||F_{meansensor}(i) - F_{sim}(i)||}{N}} \tag{8}$$

This equation for RMSE is used in the trials and this value is calculated at n^{th} sample of every trial and at every sample. N is the number of samples which in our case is 5000.

		Trials					
Error evaluation	**Axis**	**Trial 0**	**Trial 1**	**Trial 2**	**Trial 3**	**Trial 4**	**Trial 5**
Mean Error(in N)	X	0.053	0.058	0.061	0.063	0.069	0.057
	Y	0.005	0.004	0.004	0.004	0.005	0.005
	Z	0.008	0.005	0.005	0.005	0.004	0.007
RMSE(in N)	X	0.080	0.089	0.095	0.099	0.107	0.089
	Y	0.009	0.007	0.007	0.007	0.008	0.008
	Z	0.019	0.011	0.011	0.010	0.008	0.014

Table 9: Simulation trial error

6.3 Instrument deformation

To compare the tip deflection of the instrument between the simulation and the experiment, a plane is chosen since images that are compared will be in 2D and information from 2 axes can be compared. For the experimental setup, a camera is placed above the setup to be able to record the movement of the catheter through the phantom. To get the same orientation from the simulation environment, the X and Z coordinates are exported from the catheter component to a text file in order to plot the positions. The image 31 shows the orientation of the camera used during the real-life experiment.

6.3.1 Experimental deformation

9 trials were conducted to measured deformation of the catheter while being pushed through the phantom. All of these trials took the same time since actuation is used to push the catheter through the phantom. The final configuration from a random trial is shown in figure 32. The phantom is cut at the top to be able to see through it more easily in order to extract the configuration of the catheter. To compare this configuration to the simulation configuration, the phantom is used to match the sizes. The phantom is the same size in both simulation and real-life and hence, the time-step where the catheter reaches the edge of the phantom as seen in figure 32 is the same time-step in the simulation where the configuration is extracted from.

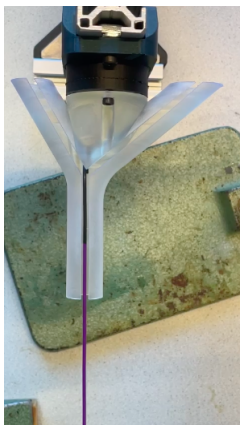

Figure 31: Camera orientation from above

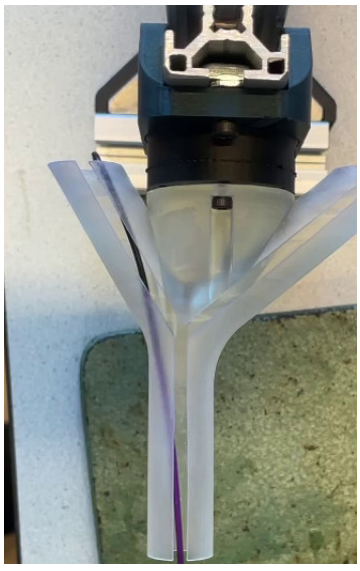

Figure 32: Final configuration(Trial 0)

6.3.2 Comparison and evaluation

The deformation measured from simulation is plotted and compared with every other trial in order to measure the error in millimeters between the tip positions. The catheters are matched with the help of the vascular phantom. By superimposing vascular phantom from the recording to the simulated image, it shows the positions of the catheters in real-world and simulation exactly against each other in the same frame since both vascular phantoms are meant to be the same size. To compare the distance between both the catheters and how accurate the simulation is, the catheter is split into 16 points. The first 7 points of these 16 points belong to the proximal part of the catheter and the last 9 points belong to the tip of the catheter. Both of these are separately compared from the images and the simulation. The image 33 shows the division of points and where they are located on the catheter. By using these points as a landmark, the same

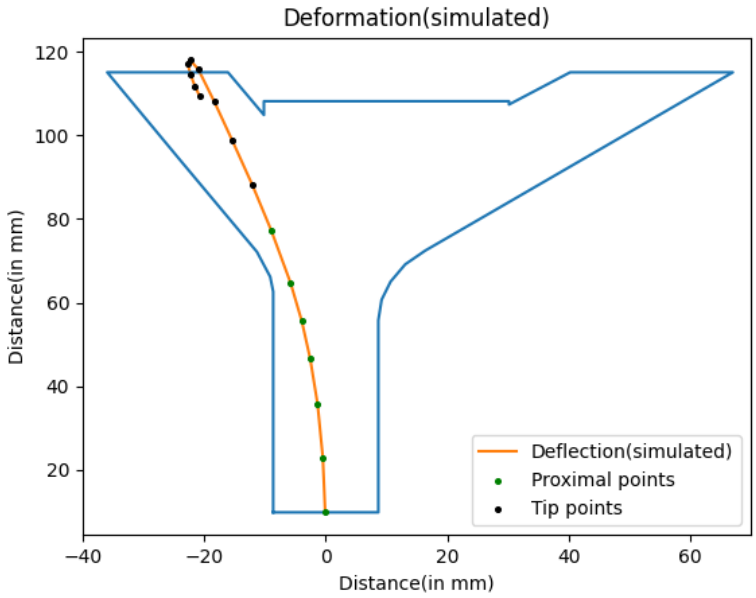

Figure 33: Simulated deformation

Y-coordinates are used for the catheter recorded from trials since they have both travelled equal distance and therefore are at the same height, therefore the same Y-coordinate. The comparison of the simulated catheter and a random trial is shown in figure 34 For each trial, the error is calculated by computing the Euclidean distance between each of these 16 points and their counterparts from the simulated catheter. For the proximal part and the tip, the error is plotted and this value is in millimeters. The mean of the error values at each node is taken from all 9 trials and this is plotted in the image 35. The RMSE[27] is

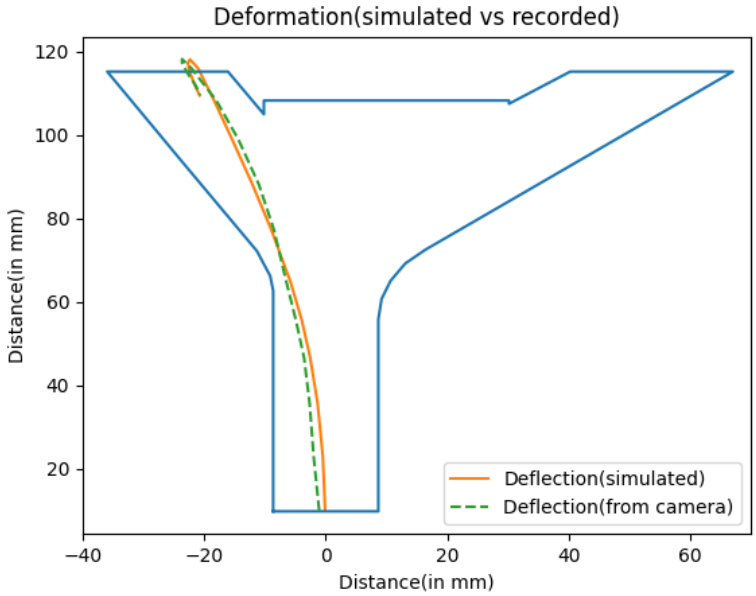

Figure 34: Deformation(simulation vs real-world)

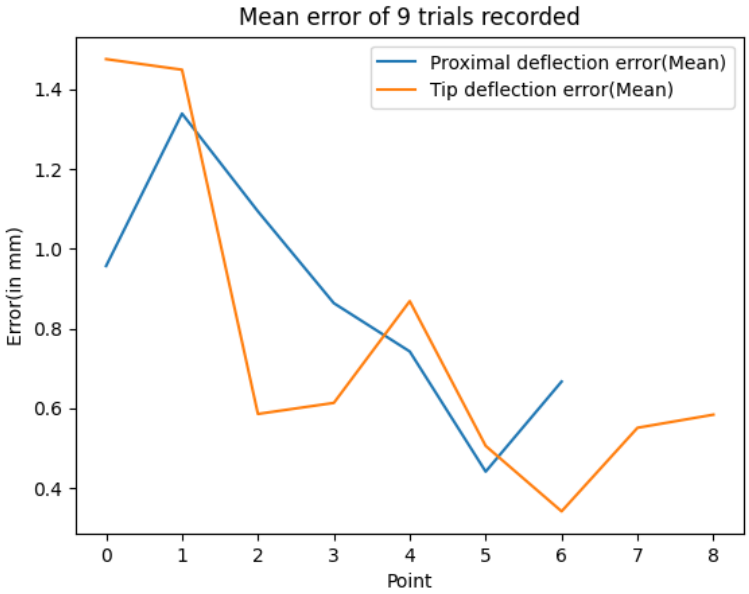

Figure 35: Mean error from 9 trials

calculated for these trials using all the formula:

$$\text{RMSE} = \sqrt{\frac{\sum_{i=0}^{8} ||d_e(i) - d_s(i)||}{9}} \tag{9}$$

Where d_e is the experimental point and d_s is the simulation point on the catheter. This is done on every point over 9 trials like in the case of mean error. RMSE over the 16 points are also plotted in a similar way and the pattern followed is exactly the same as seen in the mean error. The values seen in

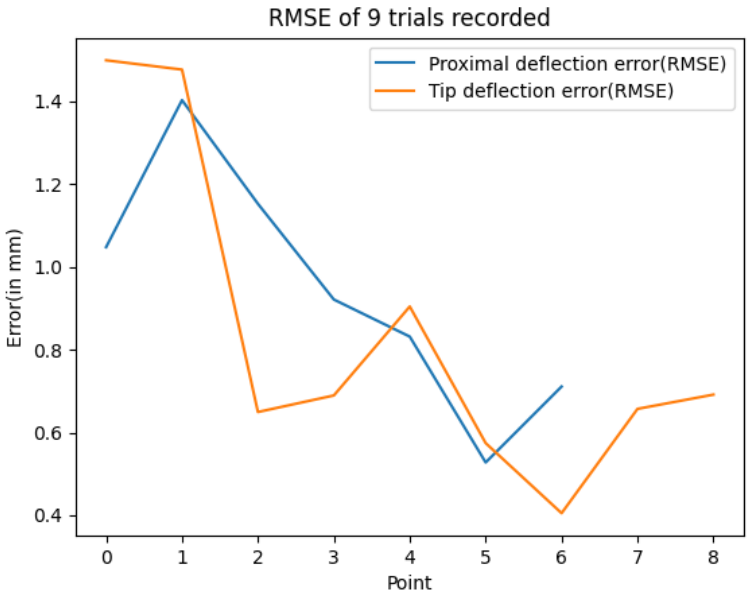

Figure 36: RMSE from 9 trials

Figures 35 and 36 are given in a table to see the values at each node and the peak values more clearly.

		Error measures	
	Nodes	**Error(Mean)(in mm)**	**Error(RMSE)(in mm)**
Proximal nodes	Node 0	0.957	1.048
	Node 1	1.339	1.403
	Node 2	1.094	1.153
	Node 3	0.864	0.921
	Node 4	0.743	0.832
	Node 5	0.442	0.528
	Node 6	0.667	0.711
Tip nodes	Node 7	1.475	1.499
	Node 8	1.449	1.477
	Node 9	0.586	0.65
	Node 10	0.614	0.69
	Node 11	0.869	0.904
	Node 12	0.506	0.574
	Node 13	0.342	0.405
	Node 14	0.552	0.657
	Node 15	0.584	0.692

Table 10: Deformation error table

7 User Interface

An implementation of a simple user interface is done to provide more options with the simulation and also customize values and choose the type of catheter that is desired to be simulated. The interface helps connect the customization to the simulation with an easier approach along with some additional features.

7.1 Customization and simulation settings

The interface provides 3 tabs out of which the first one being a tab that helps customizing the simulation parameters and provides the option of choosing the tip shape of the catheter. The first tab of the UI is shown in image 37. The settings also come with default values which were the values used for the simulation results. The dropdown box offers the choices of catheter tips. Currently, the simulator comes with 3 choices; 56535RIM, 565382CB2, 565382CB1(also known as Rim, Cobra 2 and Cobra 1). The options below the simulation settings are tickboxes which enable a specific setting. Gravity enables gravity in the simulation which changes the deformation behaviour of the catheter.

7.1.1 CathBot integration

The master manipulator of the CathBot provides values of the motor position, whether it is gripped or not and which button is activated every second at a bitrate of 1000000. With the help of this information and the position of the

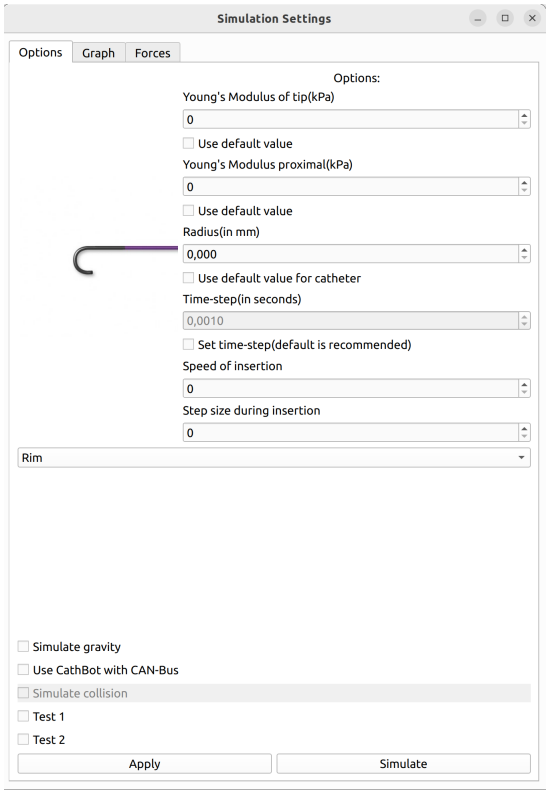

Figure 37: Simulation settings

motor, the position of the catheter in the simulation can be changed and rotated. This customizes the simulation even more and when the CathBot button is used, collision can be simulated. This is the provision of haptic feedback on the master manipulator whenever the catheter in the simulation collides with an object. Instructions to use this mode and initialize the CathBot on the simulation is given at the end. To finalize the settings, the "Apply" button has to be clicked before using the "Simulate" button.

7.2 Graph tab

This is a tab that live plots the position of the catheter from the top to be able to see the movement of the instrument when there are collisions and interactions. This can be improved to 3-D but since it is not necessary in this case, a 2-D live plot can be seen on this tab. The plotting function is shown in the image 38. This helps while using the CathBot to pilot the instrument since it tracks the whole shape from where it starts to where it moves.

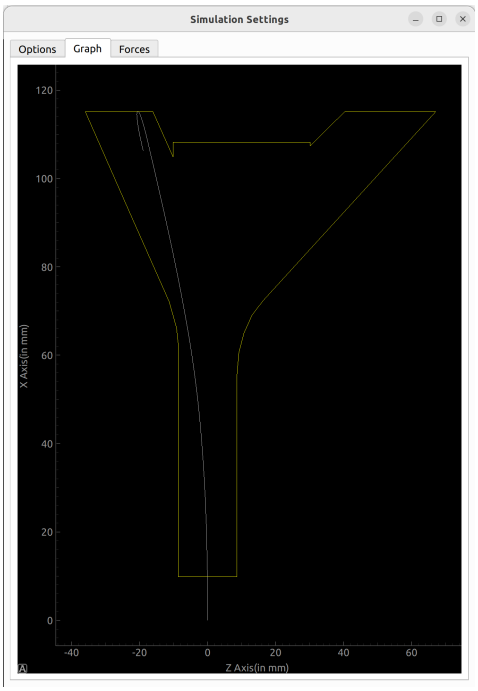

Figure 38: Catheter tracking tab

7.3 Forces tab

This is the final tab that the UI offers which live plots the forces acting on the instrument. If only one vascular phantom is used, this will give a good

estimate of contact forces since these forces will be the same force exerted by the catheter on the phantom in case of no other objects that create contact. These are plotted with the time and the limit of the timesteps can be extended or decreased based on how much is required.

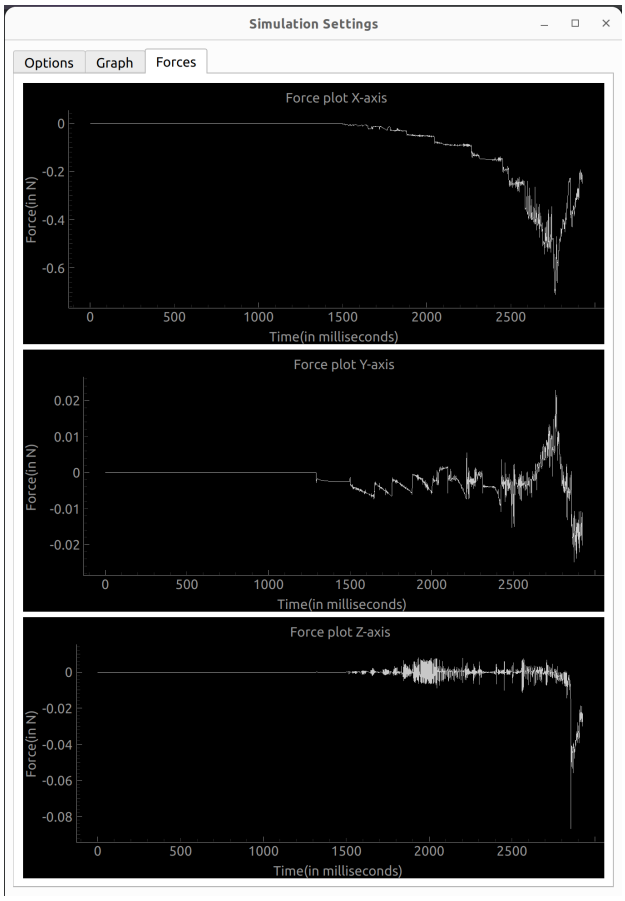

Figure 39: Contact forces in the 3 axes

7.4 User Feedback

This interface with the integration of the CathBot was tested by 7 users having 6 students and one technician who are all not experienced with surgeries. The testing included operating the CathBot in order to move the instrument in the simulation to reach target points and the tests were scored based on 6 criterion. The following box plots will show these starting with the ease to operate. The tracking accuracy describes the tracking on the interface which is shown in image 38 and the maneuverability describes how easy it is to reach wide range of

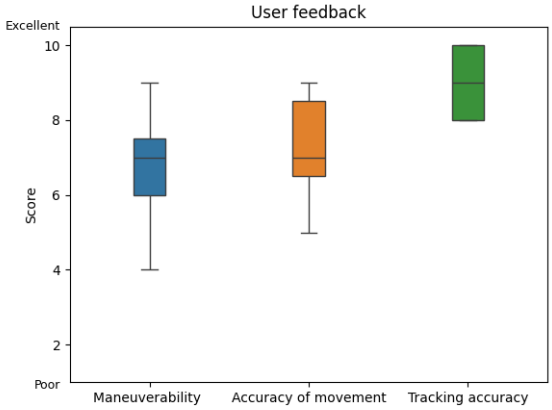

Figure 40: User feedback on CathBot integration

targets with the help of the CathBot. The accuracy of the movement describes how accurate the movement is with respect to the handling of the CathBot. Following this, the experiments and the difficulty of the tests and the delay are scored. The scores show the delay to be the main issue which also causes issues

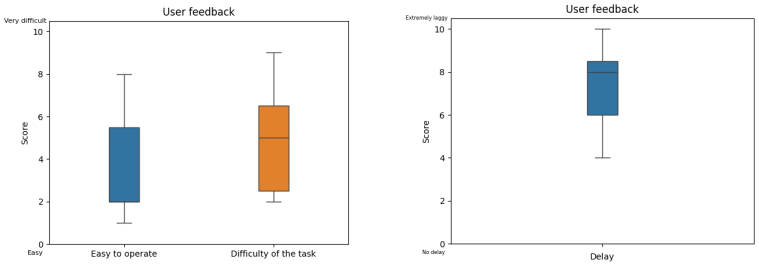

(a) Tests scoring (b) Delay

Figure 41: User feedback on testing and delay

during the use of the CathBot along with the simulation.

8 Discussion

From the force results, the force peaks are seen wherever there are more interactions with the phantom. When blood flow is considered, there will be more forces since the friction will be much higher and the navigation has to be more precise. The number of contact points is also much higher in simulation when compared to the number of contact points in the experiment. This is due to the indefinite movement in the X direction without any actual guidance. To improve this, the use of the CathBot master manipulator can help due to rotation being possible while moving through the mesh. The force estimated has some errors when contact is minimal and this is mainly due to the parameters not being exactly accurate to the materials used. The force estimation can be improved profusely by using more specific mechanical properties.

The peak force error in X-axis where most of the force is seen in the most ideal trial is about 0.23 N and the mean error is 0.053 N while the RMSE is 0.080 N. While compared to the force errors measured in Li, C. (2023) [23] where we are able to see a peaking of 0.35 N in the Z-direction which is where most contacts are as opposed to the X-direction in this case, the absolute peak is lower by a margin of 0.1 N and the mean error is around 0.034 N which is marginally lower than in our case since they are both in a very low degree of force. Although when comparing to Liu, H. (2015) [28] which uses the Cosserat Rod model to estimate forces, the maximum error as mentioned is 0.0089 N which is significantly better than here where the force estimation is done using Friction constraints in the SOFA Framework. In the paper Sayadi, A. (2021) [29], the method used to predict forces is an ANN(Artifical Neural Network) model and an SVR(Support Vector Regression) model. The mean absolute error from the ANN is 0.0217 ± 0.0191 N and the RMSE is 0.0191 N. The mean absolute error from the SVR is 0.0178 ± 0.0121 N and an RMSE of 0.0166 N. Both models are able to predict a lower error in both cases compared to the values from SOFA. This is mostly due to the models being trained with force measurements of the catheter hence being able to predict the values to a much closer extent. Another source Back, J.(2016) [30] which uses a kinematic multi section model for a catheter in order to model the shape and estimate forces is also looked into for error comparisons. The highest error is seen in Z axis where it is 0.0162 N which is also lower than the measured RMSE and Mean error here. This might be explained due to the fact that the catheters tested here are balloon catheters which are much more softer than the catheter used in our case which is a peripheral catheter used to guide guidewires. This could explain the discrepancy in errors since the peripheral catheters are made of a stronger shaft which exerts a bit more force while being used.

The mean deformation measured has a peak of 1.475mm error while the peak for RMSE is 1.499 mm which can be compared to errors measured in Li, C. (2023) [23] where the peak of tip error is around 4 mm with the mean being around 3.1 mm. While this is also lower than the measured mean error which is around 4.3

mm in the 3D image reconstruction method used by Ambrosini 2015 [31]. Since the phantom used here is much smaller than the phantom used by Li, C. [23], there are more interactions that cause more movement in the catheter. The deformation measurement from above seems to have much less error over the trials compared to the other references given following the whole body of the catheter.

The deformation error is measured throughout the body and it is noticeable that the error at the tip is much lesser compared to the body which might be due to the little discrepancy in the value of the material. The mean error over the body from both mean and RMSE errors are 0.8176 and 0.884 respectively which is less than 1 mm for the whole catheter. The model of a guidewire is tested in a paper to record deformation and compare it with their simulated guidewire. This is the source from Li, L. (2019) [32], where the average error in two specific positions are calculated to be 0.513 mm and 0.578 mm which are both lower than the average error which was mentioned above to be 0.8176 mm. The stiffness of the guidewire is higher and hence might be the reason for much lesser movement causing lesser error although it is a better performing approximation. The force measurement comes with some high errors at certain points whereas the deformation behaviour is very similar to that of the actual catheter and this can help in predicting the movement of the instrument while being used for procedures.

The force and deformation are under acceptable ranges since threshold values for force are around 1 N[33] before damage is caused to the vessel and the diameters of arteries range from 4 mm to 11.8 mm[34].

The force prediction algorithm merged with the force calculation from SOFA Framework would help reducing the error by a large extent. The forces seen while using the CathBot to move the catheter and while it is done automatically are also different since the pushing of the catheter is enabled while using the CathBot integration whereas the automatic simulation just moves in a specific direction continuously.

These values along with the behaviour of the catheter provide a very good estimate of the simulation when it comes to medical purposes. The phantoms can be tested using different catheters in order to learn which would be the best option in case of the target location. CathBot integration provides more customized movements which is how it is done in case of procedures and hence, the simulator provides a good estimate of the model along with risks and limitations.

9 Conclusions

To conclude, the experiment gives insight into how much force is actually exerted by different catheters during procedures. The threshold is around 1 N[33] on the vasculature since anything more will cause damage and possibly internal bleeding. Since the models are able to predict a value closer to the experiment while also being under the limits, this can be used as an approximate measure with respect to numbers, while the behaviour of the catheter can be a good measure due to the material properties and the physical properties. This measurement could be more accurate in the case that the parameters of the catheters are measured accurately.

The goal of this project was to design instrument models that can behave like the real-world equivalents along with a simulation environment that can be used in order to train with the CathBot where there are instruments available for the purpose of interventions and that has been fulfilled by comparisons with the actual models using different evaluation methods.

The integration of CathBot achieves the task of minimizing contacts, since movement is dependent on the user. The sensitivity is pretty moderate making it not very sensitive to touch and not very slow as well. With the availability of catheter tracking, the software provides precise location of the catheter and also giving a good estimate of what force is being exerted in which direction due to the contacts. The parameters can be completely customized making the simulator be able to serve for different catheters and also provides easy access to add various more catheters to the simulator.

9.1 Limitations and future work

With the lack of availability of accurate data, approximations had to be made to the design of the instrument. This limits the outputs and also the behaviour of the model to a certain extent. The integration of the master manipulator to the simulation also has frame drop issues since the framework is not well optimised for use of controllers and the data being sent gets delayed with the use of the software. With improvements in these fields, a much more precise simulator can be built with the use of the framework and this can assist with the use of CathBot and give a more specific measure of what to expect while using particular catheters.

The simulator can be built with more guidance and more noticeable haptic feedback since these help in improving the procedure in real-world. Control can also be applied with the help of Python on the simulation in case of a particular intervention. The model can be tested with various phantoms and blood-flow can also be an improvement since this causes a change in forces measured giving us different estimates.

The main concerns belong to the CathBot integration since the delay is noticeable and the improvement on this issue will make the simulator much more versatile for different applications and procedures. Regarding the force estimate, a neural network model that can learn from a previously available dataset and possibly multiple datasets could train it in better approximating the forces exerted which can improve the accuracy by a huge margin.

10 Bibliography

References

[1] Bourassa MG. "The history of cardiac catheterization". In: *The Canadian journal of cardiology* 21 (2005 Oct), pp. 1011–4.

[2] World Health Organization. *Cardiovascular Diseases (CVDs)*. https://www.who.int/health-topics/cardiovascular-diseases#tab=tab_1. Accessed: 2024-05-29. 2024.

[3] K. Sangeetha et al. "13 - Degradable metallic biomaterials for cardiovascular applications". In: Woodhead Publishing Series in Biomaterials (2018). Ed. by Preetha Balakrishnan, Sreekala M S, and Sabu Thomas, pp. 285–298. DOI: https://doi.org/10.1016/B978-0-08-102205-4.00013-1. URL: https://www.sciencedirect.com/science/article/pii/B9780081022054000131.

[4] Farzad Soleimani et al. "Robots and Medicine – Shaping and Defining the Future of Surgery, Endovascular Surgery, Electrophysiology and Interventional Radiology". In: *Zdravniški vestnik* 80 (Jan. 2011). DOI: 10.6016/203.

[5] M. Molinero et al. "Haptic Guidance for Robot-Assisted Endovascular Procedures: Implementation and Evaluation on Surgical Simulator". In: (Nov. 2019), pp. 5398–5403. DOI: 10.1109/IROS40897.2019.8967712.

[6] Jubo Zhao et al. "High-Precision Position Tracking Control with a Hysteresis Observer Based on the Bouc–Wen Model for Smart Material-Actuated Systems". In: *Actuators* 13.3 (2024). ISSN: 2076-0825. DOI: 10.3390/act13030105. URL: https://www.mdpi.com/2076-0825/13/3/105.

[7] Qi Yang et al. "Magnetically actuated self-clearing catheter for rapid in situ blood clot clearance for improved hemorrhagic stroke treatment". In: (Mar. 2021). DOI: 10.21203/rs.3.rs-339235/v1.

[8] Yoshinori Inoue and Koji Ikuta. "Hydraulic driven active catheters with optical bending sensor". In: (2016), pp. 383–386. DOI: 10.1109/MEMSYS.2016.7421641.

[9] Vitor Mendes Pereira et al. "Evaluation of effectiveness and safety of the CorPath GRX robotic system in endovascular embolization procedures of cerebral aneurysms". In: *J Neurointerv Surg* 16.4 (2024), pp. 405–411. DOI: 10.1136/jnis-2023-020161.

[10] NeuroNews International. *First robotic neurointervention performed with CorPath GRX system*. https://neuronewsinternational.com/first-robotic-neurointervetion/. Accessed: 2024-05-29. 2024.

[11] Emmanuel Durand et al. "Evaluation of the R-One robotic system for percutaneous coronary intervention: the R-EVOLUTION study". In: *EuroIntervention* 18.16 (2023), e1339–e1347. DOI: 10.4244/EIJ-D-22-00642.

[12] Wikipedia contributors. *Sensei robotic catheter system*. Accessed: 2024-05-29. 2024. URL: https://en.wikipedia.org/wiki/Sensei_robotic_catheter_system.

[13] Marcia K. O'Malley et al. "Expert Surgeons Can Smoothly Control Robotic Tools With a Discrete Control Interface". In: *IEEE Transactions on Human-Machine Systems* 49.4 (2019), pp. 388–394. DOI: 10.1109/THMS.2019.2919744.

[14] Dennis Kundrat et al. "An MR-Safe Endovascular Robotic Platform: Design, Control, and Ex-Vivo Evaluation". In: *IEEE Transactions on Biomedical Engineering* 68.10 (2021), pp. 3110–3121. DOI: 10.1109/TBME.2021.3065146.

[15] Yu Song et al. "Haptic feedback in robot-assisted endovascular catheterization". In: (Aug. 2017), pp. 404–409. DOI: 10.1109/ICMA.2017.8015851.

[16] Kaveh Zareinia et al. "Performance evaluation of haptic hand-controllers in a robot-assisted surgical system". In: *International Journal of Medical Robotics and Computer Assisted Surgery* 11.4 (2015). Epub 2015 Jan 27, pp. 486–501. DOI: 10.1002/rcs.1637.

[17] Jeremie Allard et al. "SOFA - an Open Source Framework for Medical Simulation". In: *Studies in health technology and informatics* 125 (Feb. 2007), pp. 13–8.

[18] Merit OEM. *56535RIM – Merit OEM Product*. https://meritoem.com/product/56535rim/. Accessed: 2024-05-29. 2024.

[19] Merit OEM. *565382CB2 – Merit OEM Product*. https://meritoem.com/product/565382cb2/. Accessed: 2024-05-29. 2024.

[20] Merit OEM. *Catheters Extrusions Diagnostic Peripheral Performa-Impress*. https://meritoem.com/wp-content/uploads/2020/11/Catheters-Extrusions_Diagnostic-Periphoral_Performa-Impress.pdf. Accessed: 2024-05-29. 2020.

[21] M Cervera et al. "Evaluation of the elastic behaviour of central venous PVC, polyurethane and silicone catheters". In: *Physics in Medicine Biology* 34.2 (1989), p. 177. DOI: 10.1088/0031-9155/34/2/002. URL: https://dx.doi.org/10.1088/0031-9155/34/2/002.

[22] LLC MatWeb. *Aluminum 6061-T6; 6061-T651*. Accessed: 2024-06-12. 2024. URL: https://www.matweb.com/search/datasheet_print.aspx?matguid=4d14eac958e5401a8fd152e1261b6843.

[23] C. Li. *Catheter modelling and force estimation in endovascular application*. 2023. URL: http://essay.utwente.nl/94002/.

[24] SOFA Consortium. *SOFA Documentation*. Accessed: 2024-05-31. 2024. URL: https://www.sofa-framework.org/community/doc.

[25] J. Lenoir C. Duriez S. Cotin and P. Neumann. "New approaches to catheter navigation for interventional radiology simulation". In: *Computer Aided Surgery* 11.6 (2006). PMID: 17458764, pp. 300–308. DOI: 10.3109/10929080601090623. eprint: https://doi.org/10.3109/10929080601090623. URL: https://doi.org/10.3109/10929080601090623.

[26] ATI Industrial Automation. *Mini40 F/T Sensor*. https://www.ati-ia.com/products/ft/ft_models.aspx?id=Mini40. Accessed: 2024-05-29. 2024.

[27] C3 AI. *Root Mean Square Error (RMSE)*. Accessed: 2024-06-12. 2024. URL: https://c3.ai/glossary/data-science/root-mean-square-error-rmse/.

[28] Junghwan Back et al. "Catheter contact force estimation from shape detection using a real-time Cosserat rod model". In: *2015 IEEE/RSJ International Conference on Intelligent Robots and Systems (IROS)*. 2015, pp. 2037–2042. DOI: 10.1109/IROS.2015.7353647.

[29] Amir Sayadi et al. "Force Estimation on Steerable Catheters through Learning-from-Simulation with ex-vivo Validation". In: *2021 International Symposium on Medical Robotics (ISMR)*. 2021, pp. 1–6. DOI: 10.1109/ISMR48346.2021.9661549.

[30] Junghwan Back et al. "New kinematic multi-section model for catheter contact force estimation and steering". In: *2016 IEEE/RSJ International Conference on Intelligent Robots and Systems (IROS)*. 2016, pp. 2122–2127. DOI: 10.1109/IROS.2016.7759333.

[31] Pierre Ambrosini et al. "Continuous roadmapping in liver TACE procedures using 2D–3D catheter-based registration". In: *International journal of computer assisted radiology and surgery* 10 (May 2015). DOI: 10.1007/s11548-015-1218-x.

[32] Long Li et al. "Investigation of Guidewire Deformation in Blood Vessels Based on an SQP Algorithm". In: *Applied Sciences* 9.2 (2019). ISSN: 2076-3417. DOI: 10.3390/app9020280. URL: https://www.mdpi.com/2076-3417/9/2/280.

[33] Linshuai Zhang et al. "A Magnetorheological Fluids-Based Robot-Assisted Catheter/Guidewire Surgery System for Endovascular Catheterization". In: *Micromachines* 12.6 (2021). ISSN: 2072-666X. DOI: 10.3390/mi12060640. URL: https://www.mdpi.com/2072-666X/12/6/640.

[34] R. Lorbeer et al. "Reference values of vessel diameters, stenosis prevalence, and arterial variations of the lower limb arteries in a male population sample using contrast-enhanced MR angiography". In: *PLoS One* 13.6 (2018), e0197559. DOI: 10.1371/journal.pone.0197559.

11 User manual

The initialization of the CathBot master manipulator in Linux requires a few drives in order to work with the interface. The connection to the PC uses a CAN-Bus interface that converts USB to CAN to the Master side. The driver used currently is an Ixxat USB-to-CAN V2 driver. The required driver is a

Figure 42: Ixxat 1.01.0281.12002 USB-to-CAN V2

modification of the driver provided on the website. This is called "Socket-CAN_2_0_378_Modified_PeWu_2022-02-11.tar" which can be downloaded from the forum provided here hms forum. After extracting this file and opening the main folder, the folder "ix_usb_can_2.0.367-MOD" has to be opened and a command prompt in this folder has to be opened as well.

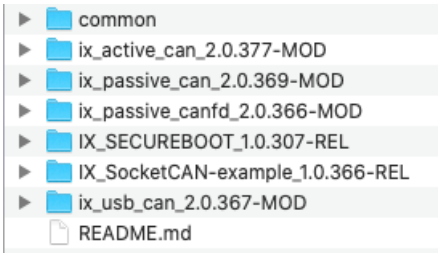

Following this, a set of commands have to be used to initialize the interface before being able to use it with Linux.

```
cmd> sudo make install
cmd> sudo ip link set can0 type can bitrate 1000000
cmd> sudo ip link set can0 up
```

After this has been done, the "Use CathBot" switch from the user interface in image 37 has to be applied and it is ready to use with the simulation software.